

RESAPLE: An Approximate One-Step Restricted Likelihood Estimator of Spatial Dependence for Exploratory Spatial Analysis

Aditya Khan^{a,b,*}, Meredith Franklin^b

^aDepartment of Computer Science, University of Toronto, 40 St George St, M5S 2E4, Toronto, ON, Canada

^bDepartment of Statistical Sciences, University of Toronto, 700 University Ave 9th Floor, M5G 1X6, Toronto, ON, Canada

ARTICLE INFO

Keywords:

Spatial Autocorrelation
Exploratory Spatial Data Analysis
Spatial Error Model

ABSTRACT

Diagnostics such as Moran's index and approximate profile likelihood-based estimators (APLE) for Gaussian spatial autoregressive models are widely used in exploratory data analysis to assess the strength of spatial dependence. Yet, although Moran's index is often applied to regression residuals, and APLE is typically formulated for raw outcomes, neither is explicitly constructed as an estimator of residual spatial dependence after adjustment for large-scale trends and covariates. We propose RESAPLE, a one-step approximate restricted maximum likelihood (REML) estimator of the spatial error model's spatial dependence parameter ρ , constructed from REML residuals. Because RESAPLE is a Rayleigh coefficient, it retains the interpretability and diagnostic convenience of exploratory indices, while also providing a computationally inexpensive and accurate estimator of ρ for moderate dependence. We show that for small to medium sample sizes and adequately specified trend models, RESAPLE is a better estimator of, and test statistic for, residual spatial dependence relative to existing alternatives including Moran's index and the APLE across a wide range of practical settings. The theory we develop also yields a diagnostic for spatial weight selection, providing guidance towards resolving a common point of ambiguity in spatial data analysis. We illustrate the method using simulations on both regular and highly irregular lattices with a case study using American Community Survey tract-level data.

1. Introduction

Spatial autoregressive (SAR) models, which include lag (SAR_{lag}) and error (SEM) specifications, are widely used to capture spatial dependence in areal (lattice) data across spatial statistics and econometrics (Zhang and Yu, 2018), with growing applications in ecology (Ver Hoef, Peterson, Hooten, Hanks and Fortin, 2018) and public health (Gao, Languille, Karzazi, Guhl, Boukebous and Deguen, 2021). Tests and estimators for spatial dependence derived from SAR and SEM models serve two complementary roles. First, they provide diagnostics for assessing model assumptions, especially violations of spatial independence, where tests of residual spatial autocorrelation are standard (Anselin, Bera, Florax and Yoon, 1996). Second, they underpin exploratory spatial data analysis (ESDA), by offering simple, interpretable, and computationally light summaries of spatial dependence or clustering in the data (Anselin, 1995).

The classical statistic for summarizing global spatial dependence is Moran's \mathcal{I}_M (Moran, 1950). Its appeal lies in its closed form expression as a ratio of quadratic forms. However, extensive work documents its shortcomings as an estimator of the spatial dependence parameter (denoted ρ). \mathcal{I}_M can be severely biased except when $\rho \approx 0$, in which case it does constitute a locally best invariant test for the parameter under appropriate conditions (Li, Calder and Cressie, 2007). Hence, Moran's \mathcal{I}_M is excellent for detection but not for estimation. This limitation motivates alternatives that preserve the interpretability of Moran's \mathcal{I}_M while more closely targeting the spatial dependence parameter, ρ .

A leading example is the approximate profile likelihood estimator (APLE) of ρ (Li et al., 2007), derived as the "one-step" (first-order) solution to the profile-likelihood score equation for ρ in a SAR model. Like Moran's \mathcal{I}_M , APLE is a closed-form ratio of quadratic forms and is straightforward to compute, making it feasible for ESDA and large datasets. Implementations are available in standard **R** packages such as `spdep`¹. Under a Gaussian model, one could always compute a maximum likelihood estimator for ρ , but that can be computationally burdensome (discussed in

*Corresponding author

✉ adityakhan@cs.toronto.edu (A. Khan); meredith.franklin@utoronto.ca (M. Franklin)

ORCID(s): 0009-0007-9798-5211 (A. Khan)

¹<https://www.rdocumentation.org/packages/spdep/versions/0.7-8/topics/aple>

Li et al. (2007)). Subsequent work has elaborated on APLE's distributional properties and extensions (see, for instance, Jin and Lee (2012); Li, Calder and Cressie (2012); Reder and Müller (2009)).

In this article we argue that despite substantial progress on APLE-type estimators, current methodology is misaligned with how practitioners actually analyse spatial regression models with covariates. In applied work, Moran's I_M and APLE are almost never computed on raw outcomes. Instead, they are used on residuals after the mean structure is removed or after detrending, either 1) implicitly, by centring variables first (as in Li et al. (2007)), or 2) explicitly, by allowing for regressors in the APLE formula (as in Li et al. (2012)).

In other words, the mismatch is that APLE is derived from the full profile likelihood, which does involve the covariates X and coefficients β , but in practice β is treated as a nuisance parameter, estimated first (typically by least squares), and only then is spatial dependence summarised on the resulting residuals. Moreover, existing APLE-type procedures with covariates can depend in non-trivial ways on how fixed effects are specified, including the particular choice of regressors and the resulting residualisation operator, even though ESDA summaries are typically intended to be stable across such choices.

Our key insight is that this tension between a joint ML for all parameters (β, ρ, σ^2) , and inference for a covariance parameter (ρ) , is exactly what REML resolves in Gaussian linear mixed models Harville (1977); Patterson and Thompson (1971). REML bases estimation of covariance parameters on linear combinations of the data that remove the fixed effects, yielding reduced bias and insensitivity to the parametrisation of the design matrix X . In the SAR/SEM setting, this perspective also yields a principled route to residual-based ESDA. Specifically, it allows spatial dependence to be summarized in the residual space after accounting for X , while preserving the computational and interpretive advantages of quadratic-form statistics.

Motivated by this, we propose RESAPLE, a REML-aligned, closed-form ESDA statistic for SEM models with covariates. RESAPLE is derived as an approximate one-step estimator from the restricted profile likelihood for ρ , and therefore matches residual practice by construction. In addition, RESAPLE is invariant to reparameterizations of X , and its curvature at the null yields an analytic information quantity that can be used to compare spatial weight matrices W in terms of local informativeness and local power for detecting spatial dependence.

The remainder of this paper is organised as follows. In Section 2, we provide some context towards the setting we work with, as well as the model definition. We then define the RESAPLE statistic in Section 3 and discuss some properties of the statistic. Then we discuss the primary use case of RESAPLE, as an ESDA statistic in Section 4. This is followed by a discussion of how the choice of spatial weight matrix, W , impacts our analysis in Section 5. We then provide a simulation study and real data case study in Section 6 and 7 respectively to empirically validate our claims. We conclude in Section 8.

2. Model Definitions and Background

We work under the Gaussian SEM. The purpose of this section is to set our notation and to introduce the residualised contrasts that underpin the definition of the RESAPLE estimator in Section 3. Let $n \in \mathbb{N}$ denote the number of spatial units, and let $p \in \{1, \dots, n-1\}$ denote the number of covariates.

2.1. Notation for the SEM

The Gaussian SEM is given by

$$Z = X\beta + U, \quad U = \rho WU + \epsilon, \quad \epsilon \sim N(0, \sigma^2 I_n). \quad (1)$$

Here, $Z \in \mathbb{R}^n$ is the observed response, $X \in \mathbb{R}^{n \times p}$ is the design matrix representing fixed effects, and $\beta \in \mathbb{R}^p$ are regression coefficients. On the error side, $W \in \mathbb{R}^{n \times n}$ is a spatial weight matrix with zero diagonal that encodes the spatial topology of the data, where w_{ij} encodes the (possibly asymmetric) proximity between locations i and j .

The scalar spatial autoregressive parameter is $\rho \in \Theta \subseteq \mathbb{R}$, where Θ is taken to be a compact subset of

$$\{\rho \in \mathbb{R} : \det R(\rho) \equiv \det(I_n - \rho W) \neq 0\}.$$

Writing $R(\rho) = I_n - \rho W$, the non-singularity condition ensures that the induced covariance structure is well defined. Further details, including the implied marginal distribution of Z and the corresponding log-likelihood, are given in Appendix A.

2.2. The Residual Space

Our estimator is constructed in the residual space obtained by removing the contribution of X . Let

$$P = X(X^\top X)^{-1}X^\top, \quad M = I_n - P.$$

Since X has full column rank p , P is a rank p orthogonal projector onto $\text{Im}(X)$, and M is the rank $n - p$ orthogonal projector onto $\text{Im}(X)^\perp$. We refer to $\text{Im}(M)$ as the residual space of the data, of dimension $r = n - p$.

Let $H \in \mathbb{R}^{n \times r}$ have orthonormal columns chosen to satisfy

$$H^\top H = I_r, \quad H H^\top = M,$$

so that the columns of H form an orthonormal basis for $\text{Im}(M) = \text{Im}(X)^\perp$. We define the residualised contrasts

$$e = H^\top Z \in \mathbb{R}^r.$$

Intuitively, e contains all information in Z that is orthogonal to the column space of X . The following lemma characterises its distribution under the SEM.

Lemma 2.1. *Under the SEM model (1),*

1. $H^\top X = 0$ and hence $e = H^\top Z = H^\top U$.
2. $e = H^\top R(\rho)^{-1}\epsilon$, and hence $e \sim N(0, \sigma^2 \Sigma_r(\rho))$ with

$$\Sigma_r(\rho) = H^\top R(\rho)^{-1} R(\rho)^{-\top} H.$$

Proof. See Appendix A. □

The distribution of e is the starting point for the derivation of the RESAPLE. The key point is that this distribution is independent of β and depends only on the covariance structure of U .

2.3. Recap of the APLE estimator

Before deriving the RESAPLE estimator, we briefly recall the APLE estimator, starting with the case where there are no covariates. The estimator is given in Li et al. (2007):

$$\hat{\rho}_{APLE} = \frac{Z^\top K Z}{Z^\top (W^\top W + v_n I_n) Z}, \quad v_n = \text{Tr}(W^2)/n, \quad K = (W + W^\top)/2.$$

This is a ratio of quadratic forms, and it is the one-step estimator

$$\hat{\rho}_{APLE} = \rho_0 - \frac{f(\rho_0)}{f'(\rho_0)} \quad (\rho_0 = 0),$$

where $f(\rho) = \frac{\partial}{\partial \rho} \ell_M^p(\rho)$ and ℓ_M^p denotes the likelihood for the data Z after profiling out σ^2 . Because it is a one-step estimator, it provides a first-order approximation to the maximum likelihood estimator while remaining in closed form. Moreover, because it is a ratio of quadratic forms, the distributional and asymptotic theory for this statistic is well developed. In particular, under a Gaussian null hypothesis $H_0 : \rho = 0$, the exact distribution of this statistic can be expressed in terms of a quadratic-form mixture of χ_1^2 variables and is numerically evaluated using Imhof's method (Imhof, 1961). In the general case where the null is $H_0 : \rho = \rho_0$, Li et al. (2007) show that a test based on APLE is first-order equivalent to a Score test and a Lagrange multiplier test, which are locally most powerful.

Later, Li et al. (2012) generalise this statistic to account for covariates, defining the updated statistic (which we refer to as MAPLE for convenience) as

$$\hat{\rho}_{MAPLE} = \frac{Z^\top M K M Z}{Z^\top (M W^\top W M - M(W^\top + W)P(W^\top W)M + v_n M) Z},$$

where the additional terms arise from incorporating covariates into the likelihood. However, despite these appealing properties, the MAPLE estimator remains an ML-based one-step approximation to the profile likelihood, and therefore

it does not align with residual-based ESDA in the presence of fixed effects. In particular, it inherits several drawbacks that are precisely those REML was designed to address. The one-step profile likelihood underlying MAPLE treats β as a nuisance parameter to be estimated by ML within the same objective. This differs from how APLE-type statistics are typically used in practice, where spatial dependence is summarised on regression residuals after removing fixed effects (Li et al., 2007). This residual-based workflow corresponds more closely to the restricted likelihood perspective than to the full ML profile likelihood.

We address these issues by defining the RESAPLE estimator in the subsequent section, as a REML-aligned closed-form statistic constructed in the residual space.

3. The RESAPLE Estimator

3.1. Defining the Estimator

We now define the RESAPLE estimator. The construction begins from the restricted profile likelihood for the residualised contrasts $e = H^\top Z$, which eliminates the regression coefficients β and bases inference for (ρ, σ^2) on the residual space. The corresponding restricted likelihood and its profiled form are given in Appendix B, together with all proofs for this section.

To motivate an estimator at $\rho = 0$, we require the restricted profile score at the null.

Lemma 3.1. *Let $\ell_r^p(\rho; e)$ denote the restricted profile log-likelihood for ρ based on e , and let $S_r(\rho) = \frac{\partial}{\partial \rho} \ell_r^p(\rho; e)$. Then the following all hold.*

1. $\Sigma_r(0) = I_r$.
2. $\Sigma_r'(0) = W_r + W_r^\top = 2K_r$, where $W_r = H^\top W H$ and $K_r = (W_r + W_r^\top)/2$.
3. Hence the restricted profile score under no spatial dependence is

$$S_r(0) = r \frac{e^\top K_r e}{e^\top e} - \text{Tr}(K_r) = r \left(\frac{e^\top K_r e}{e^\top e} - \mu_r \right), \quad (2)$$

where $\mu_r = \text{Tr}(K_r)/r$.

We now define the RESAPLE estimator. Writing

$$\mu_r = \frac{\text{Tr}(K_r)}{r}, \quad \nu_r = \frac{\text{Tr}(W_r^2)}{r},$$

we define

$$\hat{\rho}_{RESAPLE} = \frac{e^\top (K_r - \mu_r I_r) e}{e^\top (W_r^\top W_r + \nu_r I_r) e}.$$

This definition is motivated by a one-step approximation to the restricted score equation at $\rho = 0$. In addition, the trace quantity $\text{Tr}(W_r^\top W_r) + \text{Tr}(W_r^2)$ appears as the restricted Fisher information at $\rho = 0$, and therefore provides an analytic measure of local informativeness for comparing choices of W . Details are given in Appendix B.

Remark 3.2. Notice that S_r has Moran's I_M embedded into the formula, through $\frac{e^\top K_r e}{e^\top e}$, up to scaling by r , and centring by μ_r .

Theorem 3.3. *The following all hold for the RESAPLE estimator.*

1. The RESAPLE estimator is invariant to the choice of orthonormal basis H satisfying $HH^\top = M$, $H^\top H = I_r$, and $H^\top X = 0$.
2. Denote the null expectation under $\rho = 0$ as \mathbb{E}_0 . Then $\mathbb{E}_0[e^\top (K_r - \mu_r I_r) e] = 0$ and

$$\mathbb{E}_0 [e^\top (W_r^\top W_r + \nu_r I_r) e] = \sigma^2 (\text{Tr}(W_r^\top W_r) + \text{Tr}(W_r^2)) > 0$$

whenever $K_r \neq 0$.

3. The RESAPLE estimator is the one-step solution to the approximate restricted score equation

$$S_r(0) + \mathcal{I}_r^A(0)\rho = 0,$$

where

$$\mathcal{I}_r^A(0) = -\frac{r}{e^\top e} e^\top (W_r^\top W_r + v_r I_r) e$$

is an approximate restricted Fisher information (curvature) motivated by the second derivative of the restricted profile likelihood at $\rho = 0$ with σ^2 plugged in by $\hat{\sigma}_r^2(0) = \frac{1}{r} e^\top e$.

4. Consequently,

$$\hat{\rho}_{RESAPLE} = -\frac{S_r(0)}{\mathcal{I}_r^A(0)}.$$

Equivalently, $\hat{\rho}_{RESAPLE} \propto -S_r(0)/\mathcal{I}_r^A(0)$ up to multiplication of $\mathcal{I}_r^A(0)$ by a positive constant.

It is important to note that the standard APLE is a special case of the RESAPLE estimator. When X is absent ($p = 0$), we have $M = I_n$. Taking $H = I_n$ yields $r = n$, $e = Z$, and $W_r = W$. Then

$$\mu_r = \frac{\text{Tr}(W_r + W_r^\top)}{2n} = \frac{\text{Tr}(W)}{n}, \quad v_r = \frac{\text{Tr}(W_r^2)}{n}.$$

Since W has zero diagonal, $\text{Tr}(W) = 0$, and therefore

$$\hat{\rho}_{RESAPLE} = \frac{Z^\top K Z}{Z^\top (W^\top W + v_r I_n) Z},$$

which is exactly the APLE proposed in Li et al. (2007). Finally, we note that RESAPLE depends on the data only through the error contrasts e and is invariant to reparameterisations of the design matrix X . We state this as a corollary of the first point of Theorem 3.3.

Corollary 3.4. Let $\tilde{X} = XQ$ for any invertible $Q \in \mathbb{R}^{p \times p}$, and construct \tilde{H} , \tilde{e} , \tilde{W}_r , and \tilde{K}_r accordingly. Then

$$\hat{\rho}_{RESAPLE}(X) = \hat{\rho}_{RESAPLE}(\tilde{X}).$$

3.2. Properties Inherited From One-Step Estimation

It is worth emphasising that one-step estimators are well-studied, and hence, the RESAPLE inherits a number of desirable properties by virtue of being one (indeed, shared by the APLE and covariate-adjusted MAPLE estimators as well). We discuss some properties of the estimator, following van der Vaart (1998).

Recall that under the standard regularity conditions for likelihood-based estimation, a one-step estimator is asymptotically linear, and it has the same first-order asymptotic distribution as the likelihood estimator that solves the corresponding score equation. In our setting,

$$\hat{\rho}_{RESAPLE} = -\frac{S_r(0)}{\mathcal{I}_r^A(0)},$$

where $\mathcal{I}_r^A(0)$ is the (approximate) restricted curvature used for the one-step update at $\rho = 0$ (Theorem 3.3). Moreover, under mild conditions (Theorem B.6),

$$-\frac{\mathcal{I}_r^A(0)}{\mathcal{I}_r(0)} \xrightarrow{p} 1,$$

where $S_r(0)$ is defined in equation (2) and the restricted information at $\rho = 0$ is

$$\mathcal{I}_r(0) = 2 \text{Tr}(K_r^2) = \text{Tr}(W_r^\top W_r) + \text{Tr}(W_r^2)$$

(see Lemma B.4). Consequently, when ρ lies in a neighbourhood of 0 that shrinks at the \sqrt{r} scale ($r := n - p$), the RESAPLE admits a first-order expansion of the form

$$\hat{\rho}_{RESAPLE} = -\frac{S_r(0)}{\mathcal{I}_r(0)} + o_p(r^{-1/2}).$$

This immediately implies asymptotic normality if $\rho = 0$ (the reader might recognise this as a null assumption of no spatial dependence) and under local alternatives of order $r^{-1/2}$. We note that the APLE literature adopts the same one-step perspective for spatial dependence parameters (Li et al., 2007, 2012).

Second, one-step estimators inherit bias properties from Taylor expansion (see for instance Wellner). Specifically, the error in the Taylor expansion comes from higher-order derivatives of the score. Therefore, the local approximation error (and hence local bias) of the RESAPLE around a linearisation point of $\rho = 0$ is at most *quadratic* in $|\rho|$ in the \sqrt{r} -scaling. A quadratic error is negligible when ρ is small. In other words, one can treat the RESAPLE as locally *approximately* unbiased for ρ around $\rho = 0$.

It is worth bearing in mind that just as we discuss these properties of the RESAPLE, they are equally applicable to ML-based APLE-type one-step estimators. Indeed, the above arguments imply that these estimators are all asymptotically equivalent (and equivalent to full REML and ML estimation procedures for ρ) in a first-order neighbourhood around $\rho = 0$ under a \sqrt{r} -scaling. The main difference comes from the *finite-sample* case. It is in this case that the RESAPLE has the benefits that we describe earlier in this paper.

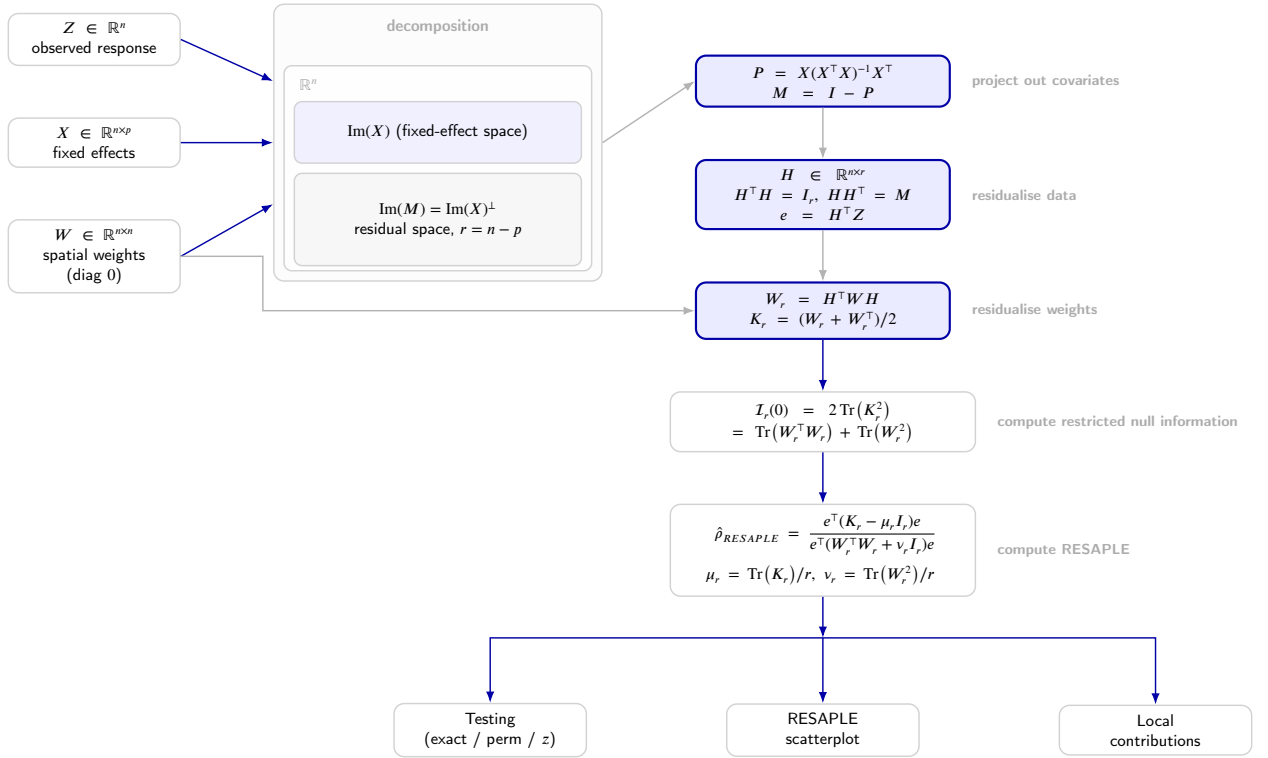


Figure 1: Overall workflow for using RESAPLE as a residual-space diagnostic for spatial dependence, in ESDA.

4. RESAPLE in ESDA

While in the previous sections, we discuss some of the baseline properties of the RESAPLE, those results primarily serve as sanity checks that the estimator we propose is well behaved. The main use case of this statistic is in ESDA, as summarized in Figure 1. We discuss three ESDA use cases of RESAPLE (i) testing for autocorrelation (as a alternative to Moran's I_M), (ii) constructing a RESAPLE scatterplot analogous to the Moran's I scatterplot, and (iii) defining a local variant of RESAPLE to diagnose local autocorrelation. A summary of the workflow is provided in Figure 1.

4.1. Testing with the RESAPLE

In many applications, the primary inferential task is to test for the presence of residual spatial autocorrelation after adjusting for covariates. In the Gaussian SEM, this leads to a hypothesis test for the spatial dependence parameter

$$H_0 : \rho = 0 \quad \text{versus} \quad H_1 : \rho > 0,$$

where the one-sided alternative reflects the usual interest in testing for positive spatial autocorrelation between neighbouring areal units. In general, practitioners default to Moran's \mathcal{I}_M computed on unadjusted data or on regression residuals. For Gaussian SAR or SEM models without covariates, and under suitable regularity conditions, it is rather well-known that \mathcal{I}_M yields a locally most powerful invariant test for $H_0 : \rho = 0$ against local alternatives in which ρ is small and positive (discussed for instance in Li et al. (2007)). However, it is well documented that Moran's \mathcal{I}_M is severely biased as an estimator of ρ away from the null and that its finite sample distribution can differ markedly from its asymptotic approximation, especially in the presence of covariates and pathological spatial weight matrices that can be induced by adjacency (also in Li et al. (2007)). In particular, when covariates are present, the usual procedure of computing Moran's \mathcal{I}_M on residuals obtained from a fixed effects model is not aligned with the likelihood for ρ and does not account for the contribution of X to the covariance structure.

The RESAPLE framework we propose provides a natural alternative test statistic that is constructed in the residual space and is directly linked to the restricted likelihood. In what follows (Figure 1), we regard the RESAPLE estimator as the basic test statistic for $H_0 : \rho = 0$. There are three potential ways to test with $\hat{\rho}_{RESAPLE}$:

1. exact testing,
2. permutation testing, and
3. (approximate) z-testing.

We discuss each method and their benefits and drawbacks in turn.

Exact testing under a Gaussian null. Assume the Gaussian SEM and $H_0 : \rho = 0$. Lemma 2.1 implies $e = H^\top Z \sim N(0, \sigma^2 I_r)$ with $r = n - p$. Under this null, $\hat{\rho}_{RESAPLE}$ is a ratio of quadratic forms in a Gaussian vector, so one can evaluate its null distribution using classical methods for quadratic forms in normal variables. In particular, for any observed value $t \in \mathbb{R}$,

$$\mathbb{P}_0(\hat{\rho}_{RESAPLE} \geq t) = \mathbb{P}_0(e^\top (A_t) e \geq 0), \quad (3)$$

where A_t is a deterministic symmetric matrix depending on t , W_r , and K_r . After diagonalising A_t , we can show that the quadratic form $e^\top A_t e$ is just equal in distribution to a finite weighted sum of independent χ_1^2 variables. Numerical computation of the tails is standard in the literature (e.g. Imhof (1961)). If the assumed model is correct, this is exact. But it is not robust to violations of the model assumptions. Furthermore, using this test requires an eigendecomposition of a matrix of dimension r , and its numerical cost can therefore be non-trivial when r is large.

Permutation testing. If we wish to avoid over-reliance on this distributional assumption, we can instead use a randomisation approach. Under H_0 in the Gaussian SEM, Lemma 2.1 implies $e \sim N(0, \sigma^2 I_r)$, and hence the coordinates of e are exchangeable in any fixed orthonormal basis of the residual space. This motivates a permutation test that recomputes $\hat{\rho}_{RESAPLE}$ on permuted contrasts Πe over many randomly sampled permutation matrices $\Pi \in \mathbb{R}^{r \times r}$, and compares the observed statistic to the resulting randomisation distribution. Since the statistic $\hat{\rho}_{RESAPLE}$ is invariant to the choice of H (Theorem 3.3), but the permutation operation acts on the coordinates of e and therefore depends on the chosen contrast basis, we make the procedure unambiguous by taking H to be the orthonormal complement obtained from a QR decomposition of X , and we then define $e = H^\top Z$ and permute its coordinates. An alternative residual-based randomisation strategy is the Freedman-Lane procedure (Freedman and Lane, 1983), which permutes residuals from the reduced model under H_0 and reconstructs pseudo-responses before recomputing the statistic. Both approaches are natural in this setting; in our simulation experiments, we use the Freedman-Lane procedure for calibration. The permutation approach is straightforward to implement and avoids heavy eigendecompositions. It can, however, require many permutations for stable tail probability estimation.

Approximate z-testing. Finally, one may appeal to the asymptotic normal approximation implied by the one-step construction, discussed in section 3.2. This motivates us to use the test statistic

$$Z_{RESAPLE} = \sqrt{\mathcal{I}_r(0)} \hat{\rho}_{RESAPLE}, \quad \mathcal{I}_r(0) = \text{Tr}(W_r^\top W_r) + \text{Tr}(W_r^2),$$

and compare $Z_{RESAPLE}$ to the upper tail of a standard normal distribution under H_0 . This method is of course, computationally simple.

Each of these three methods has their benefits and drawbacks. It is worth briefly commenting on the alternatives to RESAPLE. As has been the theme in this paper, tests based on RESAPLE are better aligned with covariate adjusted workflows than APLE or MAPLE. The main concern the reader may have though, is why not simply use a likelihood ratio statistic derived from the restricted likelihood for the SEM, which compares the restricted likelihood maximised under $\rho = 0$ to that maximised over $\rho \in \Theta$ (Anselin, 1988)? It is true that this approach is appealing when one intends to fit the SEM by REML in any case. It can, however, be computationally burdensome in large problems, since it requires repeated evaluation of $\log |R(\rho)|$ and numerical optimisation over ρ . In the ESDA setting where one seeks an exploratory check, RESAPLE remains low-cost while just as accurate as REML asymptotically, and accurate for small ρ (which is typically the regime one would wish to test autocorrelation for—when autocorrelation is not exactly obvious).

4.2. Scatterplot Diagnostics

Scatterplots are central tools in ESDA because they provide a direct visual decomposition of global spatial association into unit-level contributions. The classical example is the Moran scatterplot, which plots a residual (resp. centred data) against a spatially lagged residual (resp. centred data). In its standard form, the slope of the fitted line through the origin equals Moran's I_M , and the four quadrants of the plot identify high-high, low-low, high-low, and low-high patterns of local autocorrelation. This diagnostic is primarily a tool for detecting spatial dependence in data, in the sense that it visualises the quadratic form $e^\top K_r e$ (or its centred variant).

In this subsection we develop a RESAPLE analogue of the Moran scatterplot and of the APLE scatterplot, as illustrated schematically in Figure 2. The main idea here is that statistics of the form

$$\frac{e^\top A e}{e^\top B e},$$

with A symmetric and B positive definite, define a generalised Rayleigh quotient. Such a ratio admits a canonical regression interpretation after a whitening transformation determined by B . This yields a scatterplot whose ordinary least squares slope through the origin equals the ratio itself, and whose residuals provide a diagnostic for how well the implied one-dimensional summary represents the transformed contrasts. When applied to Moran-type statistics, this reproduces the classical Moran scatterplot (Anselin et al., 1996), as with the APLE scatterplot when applied to APLE statistics (Li et al., 2007). Of course, when we apply it to the RESAPLE, we continue to get a scatterplot whose slope equals $\hat{\rho}_{RESAPLE}$, but the key distinction is that the axes of the scatterplot are defined intrinsically in the restricted residual space.

To construct the scatterplot, recall that

$$\hat{\rho}_{RESAPLE} = \frac{e^\top A_r e}{e^\top B_r e}.$$

with

$$A_r := K_r - \mu_r I_r, \quad B_r := W_r^\top W_r + \nu_r I_r.$$

Then A_r is symmetric. Provided that B_r is symmetric, positive definite (this matter is discussed in Remark 4.1), define the whitened contrasts $x, y \in \mathbb{R}^r$ by

$$x := B_r^{1/2} e, \quad y := B_r^{-1/2} A_r e. \tag{4}$$

Then

$$x^\top x = e^\top B_r e, \quad x^\top y = e^\top A_r e.$$

A straightforward calculation shows then that the ordinary least squares slope through the origin in the regression of y on x equals

$$\frac{x^\top y}{x^\top x} = \frac{e^\top A_r e}{e^\top B_r e} = \hat{\rho}_{RESAPLE},$$

which is the standard regression interpretation used in Moran and APLE scatterplots (Anselin et al., 1996; Li et al., 2007). The key idea here is that the vectors x and y live in the residual space \mathbb{R}^r and *not* in the fixed-effect space. To

obtain unit-level coordinates indexed by the original spatial units, define

$$\tilde{x} := Hx = HB_r^{1/2}e, \quad \tilde{y} := Hy = HB_r^{-1/2}A_re. \quad (5)$$

We refer to the components $(\tilde{x}_i, \tilde{y}_i)$ for $i \in \{1, \dots, n\}$ as the plotted coordinates. Since $H^T H = I_r$, these satisfy

$$\sum_{i=1}^n \tilde{x}_i^2 = \tilde{x}^T \tilde{x} = x^T x = e^T B_r e, \quad \sum_{i=1}^n \tilde{x}_i \tilde{y}_i = \tilde{x}^T \tilde{y} = x^T y = e^T A_r e.$$

Consequently,

$$\hat{\rho}_{RESAPLE} = \frac{\sum_{i=1}^n \tilde{x}_i \tilde{y}_i}{\sum_{i=1}^n \tilde{x}_i^2}. \quad (6)$$

In other words, equation (6) provides a direct decomposition of $\hat{\rho}_{RESAPLE}$ into unit-level contributions $\tilde{x}_i \tilde{y}_i$, with weights determined by \tilde{x}_i^2 (Figure 2).

It is worth noting that RESAPLE scatterplot provides information that Moran and APLE scatterplots do not provide when covariates are present. First, the construction in (5) depends on (X, W) through the restricted operators (W_r, K_r) , so the plot reflects the interaction between the spatial topology and the residual space after adjusting for the covariates, X . This differs from the Moran scatterplot computed on raw data, and (more importantly) it also differs from the practice of plotting a residual against a spatial lag of that residual, which does not incorporate the restricted operators that come from the restricted likelihood. Second, the denominator $e^T B_r e$ in (6) is obtained from the RESAPLE construction and connects to the curvature quantities such as $\mathcal{I}_r(0)$. The terms in the denominator of (6) (i.e. \tilde{x}_i^2), therefore identify spatial units that contribute strongly to this curvature in the residual space. This yields a diagnostic for where the information about ρ concentrates after adjusting for X , which the Moran and APLE scatterplots do not directly display.

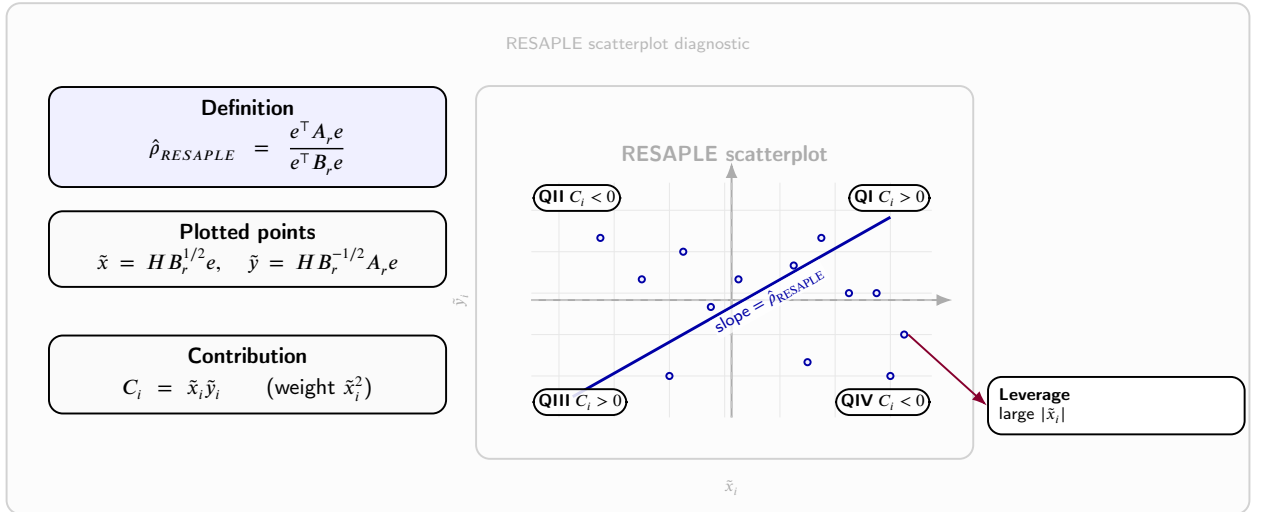


Figure 2: Schematic RESAPLE scatterplot. The slope equals $\hat{\rho}_{RESAPLE}$. Unit contributions are $C_i = \tilde{x}_i \tilde{y}_i$ with leverage proportional to \tilde{x}_i^2 .

Remark 4.1. The RESAPLE scatterplot construction in (4) uses the matrix $B_r := W_r^T W_r + \nu_r I_r$ and therefore requires $B_r > 0$ to define $B_r^{\pm 1/2}$. While $W_r^T W_r \geq 0$ always, the scalar $\nu_r = \text{Tr}(W_r^2)/r$ is not guaranteed to be nonnegative for an arbitrary (non-symmetric) residualised operator $W_r = H^T W H$, and hence B_r need not be positive definite in full generality. In the important special case of symmetric weights (e.g. undirected graphs with symmetric normalisation), W_r is symmetric and $\nu_r = \text{Tr}(W_r^2)/r = \|W_r\|_F^2/r \geq 0$, so $B_r > 0$ whenever $W_r \neq 0$. For general (possibly non-symmetric) weights, the RESAPLE point estimator $\hat{\rho}_{RESAPLE} = (e^T A_r e)/(e^T B_r e)$ remains well-defined whenever $e^T B_r e > 0$. If that fails, we replace B_r by the stabilised denominator $\tilde{B}_r := W_r^T W_r + \tilde{\nu}_r I_r$, $\tilde{\nu}_r := \text{Tr}(W_r^T W_r)/r$. Then

$\tilde{B}_r > 0$ whenever $W_r \neq 0$. In the symmetric case, $\tilde{v}_r = v_r$, so this modification leaves the construction unchanged. This stabilisation only affects the denominator by an isotropic nonnegative term. This stabilised denominator may also be used in the Gaussian exact test discussed in Section 4.1.

4.3. Local Testing

So far we have been working with global ESDA summaries, which are primarily designed to detect or quantify dependence aggregated over the entire spatial domain. In practice, dependence in the data is usually spatially heterogeneous, with clustering that often is not well captured by global statistics. This motivates the use of local indicators of spatial association, where each spatial unit is assigned a local statistic whose extremes identify candidate hot spots in the data. The classical example is the local Moran statistic in Anselin (1995).

Just as one can construct a local Moran statistic, one can do the same for the RESAPLE. However the key distinction from classical local Moran diagnostics (as with local APLE) is conceptual. Local Moran statistics provide a local assessment of spatial association in the original data or residual scale (Anselin, 1995). In contrast, the RESAPLE is a ratio in the residual space.

Recall that the RESAPLE can be written as a weighted sum of local contributions, as in (6). This motivates a local contribution statistic in the form

$$C_i := \tilde{x}_i \tilde{y}_i, \quad i \in \{1, \dots, n\}. \quad (7)$$

The sign of C_i indicates whether unit i contributes positively or negatively to the global numerator $e^\top A_r e$, and its magnitude determines the strength of the contribution. Since the denominator in (6) is positive, units with large positive C_i push $\hat{\rho}_{RESAPLE}$ upward, while units with large negative C_i push $\hat{\rho}_{RESAPLE}$ downward.

Further, if we normalise the local contributions by the global denominator and define

$$S_i := \frac{C_i}{\sum_{j=1}^n \tilde{x}_j^2} = \frac{\tilde{x}_i \tilde{y}_i}{e^\top B_r e}, \quad (8)$$

this normalisation yields $\sum_{i=1}^n S_i = \hat{\rho}_{RESAPLE}$, so S_i provides a direct unit-level decomposition of the RESAPLE itself.

Clearly, the local statistics have a close connection to the RESAPLE scatterplot. This can be seen by partitioning the scatterplot units into four quadrants according to the signs of $(\tilde{x}_i, \tilde{y}_i)$, essentially like the Moran scatterplot (Anselin et al., 1996). Units in the first and third quadrants satisfy $C_i > 0$ and contribute positively to RESAPLE, just as units in the second and fourth quadrants satisfy $C_i < 0$ and contribute negatively.

Beyond the interpretation of the local RESAPLE statistics in terms of the scatterplot, we can also define local tests (just as there are local tests defined based on the local Moran statistics). The procedure of testing by permutation is essentially identical to the procedure for the global RESAPLE statistic. The key distinction is that to control the family-wise error rate or the false discovery rate (generally the latter in ESDA), one must conduct multiple testing corrections.

5. Impact of the Choice of W

Throughout this paper, we have been ignoring the important role that the choice of W plays. Indeed, a central practical difficulty in spatial regression is that the spatial weight matrix W is rarely determined uniquely by the research problem. In many applied analyses, one can envision the data analyst beginning with a family of plausible neighbourhood structures, and then selecting one weight matrix as a compromise between interpretability and power (Anselin, 1988). We can formalise this by defining a candidate class of plausible weight matrices that faithfully describe the spatial topology,

$$\mathcal{W} \subseteq \mathbb{R}^{n \times n},$$

where \mathcal{W} may include, for example, contiguity-based weights such as rook or queen adjacency, k nearest neighbour weights, or distance-band weights.

Very often, there are two considerations the hypothetical data analyst has to consider. First, there is the question of neighbourhood size. Increasing the number of neighbours reduces variance in the spatial lag, but it also changes the scale of W under standard normalisations, and it can affect boundary behaviour. In particular, for row-standardised weights, boundary units with fewer neighbours receive larger per-neighbour weights, which may amplify edge effects.

Second, there is the question of regularity. Weight matrices arising from regular lattices yield stable spectral behaviour, while highly irregular spatial graphs can lead to heavy-tailed or multimodal finite-sample distributions for quadratic-form diagnostics. This issue is emphasised in Reder and Müller (2009), who examine a collection of maximally connected planar structures (the B-series) with fixed size $n = 8$ and fixed overall connectivity, and report that for certain irregular structures, the APLE loses its empirical advantage over Moran-type diagnostics at moderate dependence levels, exhibiting both appreciable bias and increased variance when ρ is not close to 0.

The statistic that one needs to understand the local behaviour of the RESAPLE is the restricted information at the null, which, as shown in Lemma B.4, satisfies

$$\mathcal{I}_r(0) = \text{Tr}(W_r^\top W_r) + \text{Tr}(W_r^2) = 2 \text{Tr}(K_r^2).$$

It follows from local asymptotic theory that the local asymptotic power of likelihood based tests tracks the Fisher information (van der Vaart, 1998). Within a candidate class \mathcal{W} , weight matrices with larger $\mathcal{I}_r(0)$ yield greater local power. In other words, $\mathcal{I}_r(0)$ gives an analytic measure of detectability for spatial dependence using RESAPLE.

It is also true that neighbourhood size and edge effects can be related analytically to $\mathcal{I}_r(0)$ for common choices of weight matrix. One widely used choice is row-standardised contiguity weights derived from a binary adjacency matrix. The following result expresses $\mathcal{I}_r(0)$ in terms of the out-degrees of the areal units.

Theorem 5.1. *Let $A \in \{0, 1\}^{n \times n}$ be a directed adjacency matrix with zero diagonal and out-degrees $d_i := \sum_{j=1}^n a_{ij} > 0$. Let $D = \text{diag}(d_1, \dots, d_n)$ and $W = D^{-1}A$. Let $M = I_n - X(X^\top X)^{-1}X^\top$ and let $K = (W + W^\top)/2$. Then the restricted information at $\rho = 0$ satisfies*

$$\mathcal{I}_r(0) = 2 \text{Tr}(K_r^2) = 2 \text{Tr}(M K M K), \quad (9)$$

and, in particular,

$$\mathcal{I}_r(0) \leq 2 \text{Tr}(K^2) = \text{Tr}(W^\top W) + \text{Tr}(W^2). \quad (10)$$

Moreover, for row-standardised adjacency weights,

$$\text{Tr}(W^\top W) = \sum_{i=1}^n \frac{1}{d_i}, \quad \text{Tr}(W^2) = \sum_{i=1}^n \sum_{j=1}^n \frac{a_{ij} a_{ji}}{d_i d_j}. \quad (11)$$

If A is symmetric, then $\text{Tr}(W^2) = 2 \sum_{\{i,j\} \in E} (d_i d_j)^{-1}$, with E the set of edges. If, further, the graph is d -regular, then $\text{Tr}(W^\top W) + \text{Tr}(W^2) = 2n/d$.

The bound (10) and the identities (11) give us two immediate qualitative consequences for row-standardised weights. First, the term $\sum_i d_i^{-1}$ increases when the graph contains many low-degree nodes, which occurs naturally at boundaries for contiguity graphs. If the inequality (10) is relatively tight, then this shows that the boundary areal units disproportionately impact the unrestricted information and hence RESAPLE statistic, compared to interior nodes. This is an analytic proof of what is known as *edge effects* in spatial statistics. In general, the identities (11) also show that uniformly increasing degrees d_i decrease the Fisher information, which generally decreases detectability of spatial dependence, making the test less powerful.

Beyond just changing the information, irregular spatial topologies induced by binary contiguity can also change the shape of the sampling distribution of the RESAPLE. To study this phenomenon, suppose for a moment that the residual contrasts e are Gaussian in \mathbb{R}^r . In this case, noting that the RESAPLE is a Rayleigh coefficient, one can show that its distribution is determined exactly by an appropriately defined spectrum of eigenvalues. When r is small, or when eigenvalues in the spectrum have large multiplicities, the resulting distribution can deviate strongly from a Gaussian approximation. This observation provides a theoretical explanation for the type of phenomena reported in Reder and Müller (2009) for the B-series graphs, and it motivates the use of exact null reference distributions or permutation in small and irregular settings. A heuristic rationale for this is given by Theorem D.1 in Appendix D.

In summary, the choice of W affects RESAPLE in two ways. It affects the restricted information $\mathcal{I}_r(0)$, which controls local power and local precision near $\rho = 0$. It also affects its distributional shape through the spectrum of residualised operators such as K_r , which becomes particularly relevant in small samples and irregular neighbourhood structures. The key idea here is that when ρ is expected to be close to 0 and r is moderate to large, Theorem 5.1 suggests that $\mathcal{I}_r(0)$ provides a principled way to compare candidate weights for local detectability. In settings where r is small with high eigenvalue multiplicities, exact testing is a better option than approximate z-testing with RESAPLE.

Factor	Values in Simulation 1
Topological structure	Queen contiguity ($m \times m$ lattice); B07
Sample size (queen)	$n \in \{25, 100, 400\}$ with $m \in \{5, 10, 20\}$ and $n = m^2$
Sample size (B07)	$n = 8$
Covariate dimension (queen)	$p \in \{1, 5, 20\}$ subject to $p < n$
Covariate dimension (B07)	$p \in \{1, 3, 5\}$ subject to $p < n$
Dependence strength	$\rho \in \{0, 0.05, \dots, 0.95\}$
Noise scale	$\sigma = 1$
Monte Carlo replicates	$K = 2000$ per design point

Table 1

Simulation 1 design. The restriction $p < n$ ensures a non-trivial residual space and avoids rank deficiencies in residualisation.

6. Simulation Study

Now, we conduct a simulation study to evaluate RESAPLE and its properties. First, we quantify bias and variability for RESAPLE and its comparators. Secondly, we assess empirical size and power for the null $H_0 : \rho = 0$. Thirdly, we examine how properties of the weight matrix W and of the underlying geometry influence the ability to detect significant spatial dependence. Implementation details, including specifications for weight matrices, covariates, and coefficients, are provided in Appendix E. For all tests, we fix $\alpha = 0.05$ throughout.

6.1. Simulation 1: Behaviour of RESAPLE as a Point Estimator

In the first simulation, we study the RMSE of RESAPLE and several of its alternatives (Moran's I_M , APLE computed on residuals, MAPLE, and REML) against a true $\rho \in \{0, 0.05, 0.10, \dots, 0.90, 0.95\}$ across a variety of different scenarios, primarily by Monte Carlo ($K = 2000$ replicates, which is sufficient since the summaries we study for this simulation are smooth averages).

In particular, for each simulation setting (which we call a design point), data are generated from a Gaussian SEM. The factorial design is summarised in Table 1. We fix the noise scale at $\sigma = 1$ so that comparisons across design points are not confounded by variance rescaling. Throughout, W is row-standardised so that each row sums to one, which places ρ on a comparable scale across topologies and sample sizes.

The Queen lattice setting demonstrates a common spatial topology that practitioners often use. To explore the impact of a more pathological topology, we also examined a B07 pattern, which is a small highly irregular adjacency graph (as in Reder and Müller (2009)). The three values of p ($p = 1, 5, 20$ for queen; $p = 1, 3, 5$ for B07) span an intercept-only specification, a moderate covariate adjustment, and a higher-dimensional adjustment that reduces residual degrees of freedom, r .

The simulations show that for almost all design points, RESAPLE achieves the lowest RMSE (and hence best balance of bias and variance), which is particularly notable for larger ρ (Figure 3). For the queen contiguity, RESAPLE shows notably lower RMSE compared to MAPLE and APLE when the sample size is small ($n = 25$). As the sample size grows there is less distinction between the methods. Furthermore, the the shape of the RMSE trend curve as ρ gets larger is very similar as sample size increases. When $r = n - p$ is small we see some instability in the performance of RESAPLE—for instance, the queen contiguity when p is large and ρ is small (Figure 3a) and the B07 contiguity when p is moderate and ρ is small (Figure 3b).

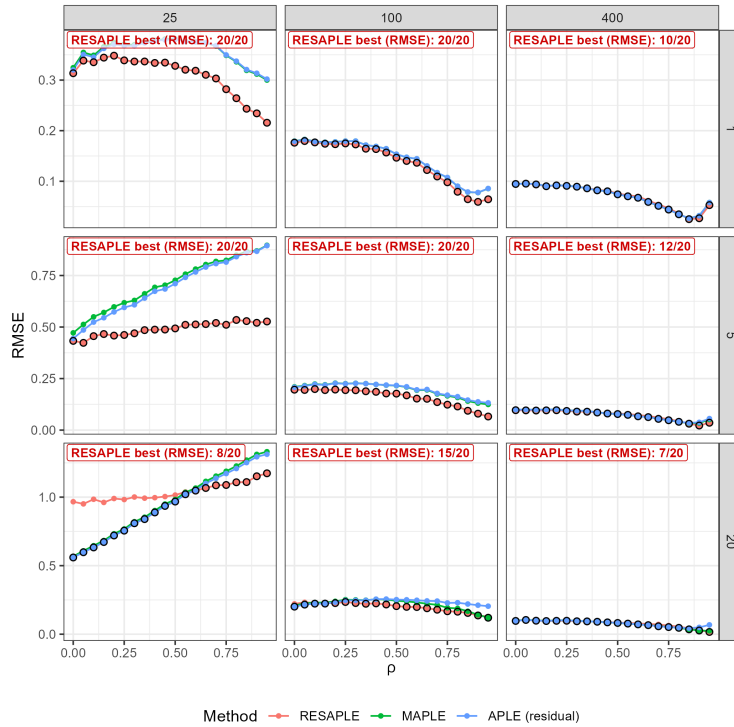
Despite RESAPLE having the best *tradeoff* between variance and bias (as reflected by its low RMSE), this advantage is driven primarily by reduced *bias*. We observe that RESAPLE often has the largest sampling variability ($SD \approx \sqrt{RMSE^2 - Bias^2}$) among the three estimators (Figure 4), particularly when n is small. However, as n increases, its variability becomes comparable to the alternatives while its bias remains substantially lower. Overall, RESAPLE appears to be a robust choice when n is larger and the residual degrees of freedom $r = n - p$ remain reasonably large, including settings with larger p .

6.2. Simulation 2: RESAPLE as a Test Statistic

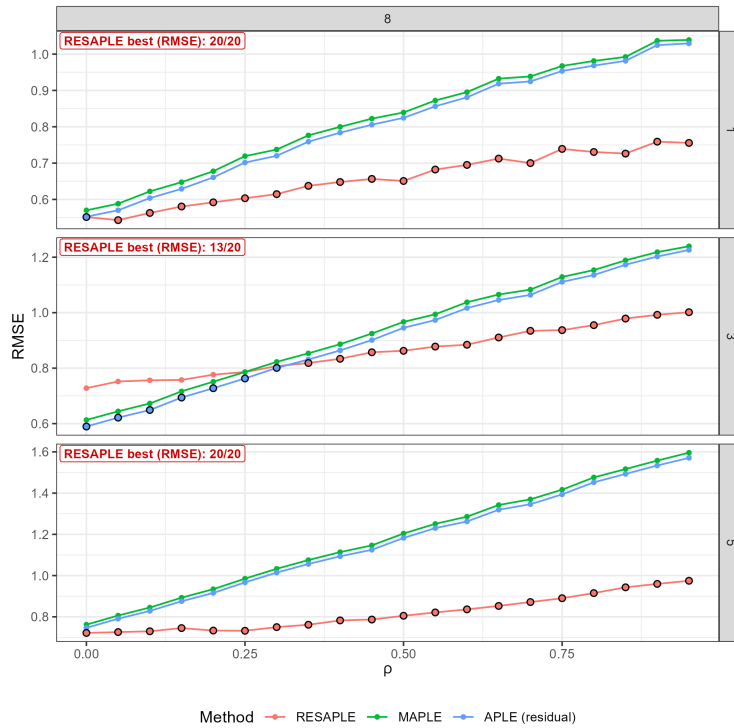
In this simulation, we evaluate RESAPLE as a test statistic for residual spatial autocorrelation using the two-sided hypothesis test

$$H_0 : \rho = 0 \text{ versus } H_1 : \rho \neq 0$$

RESAPLE



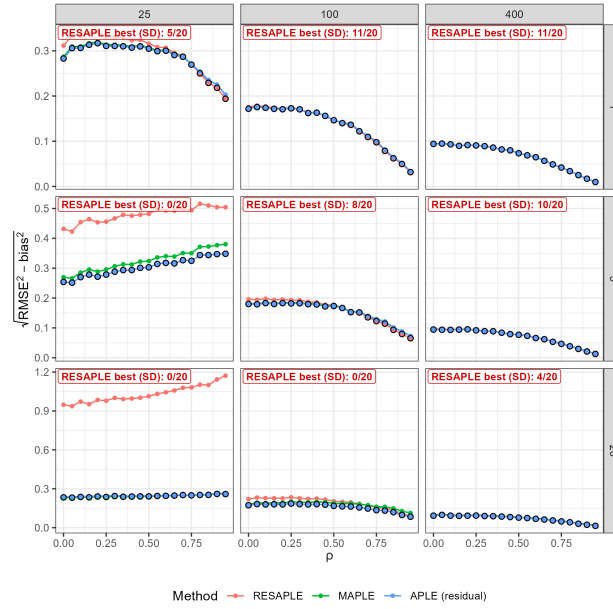
(a) RMSE against ρ on Queen contiguity.



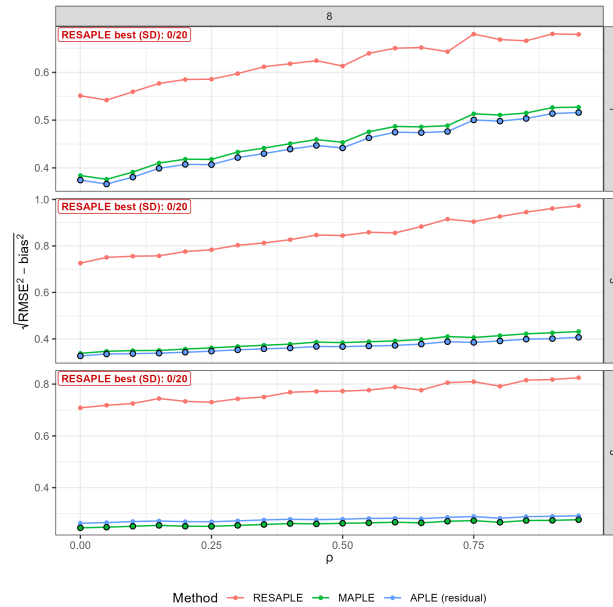
(b) RMSE against ρ on B07.

Figure 3: RMSE against ρ . $K = 2000$ MC replicates. Faceted by n (horizontal) and ρ (vertical). For each design point, for each of the 20 values of ρ (from 0 to 0.95), we count and annotate how many times RESAPLE attains the best RMSE.

RESAPLE



(a) Sampling Variability of Estimators on Queen.



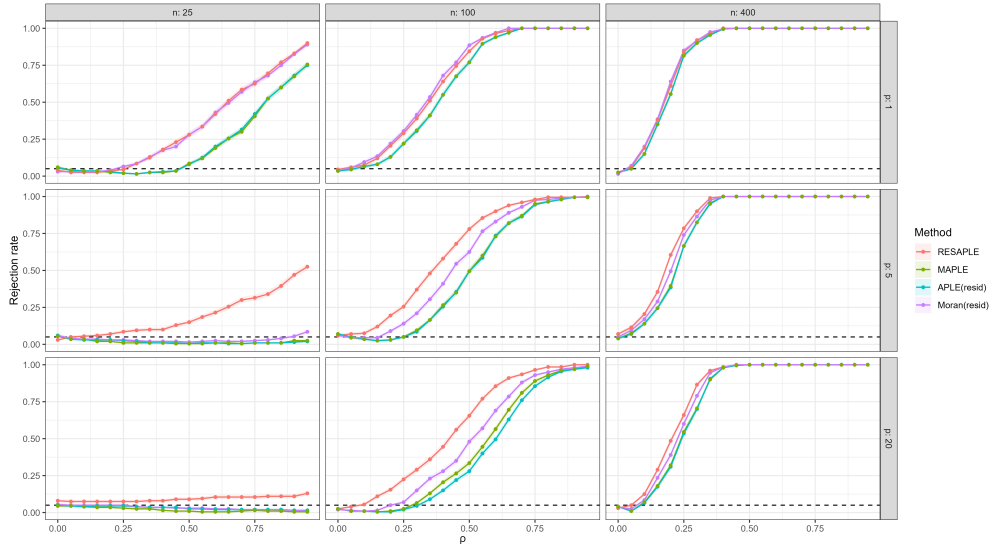
(b) Sampling Variability of Estimators on B07.

Figure 4: Simulation results of the RESAPLE, MAPLE, and APLE (residual) sampling standard deviation represented by $\sqrt{\text{RMSE}^2 - \text{Bias}^2}$ versus spatial autocorrelation ρ (from 0 to 0.95) calculated on $K = 2000$ MC replicates for (a) queen contiguity and (b) B07 contiguity. The plots are faceted by sample size n (horizontal) and number of covariates p (vertical), and are annotated with how many times RESAPLE had the lowest sampling variability.

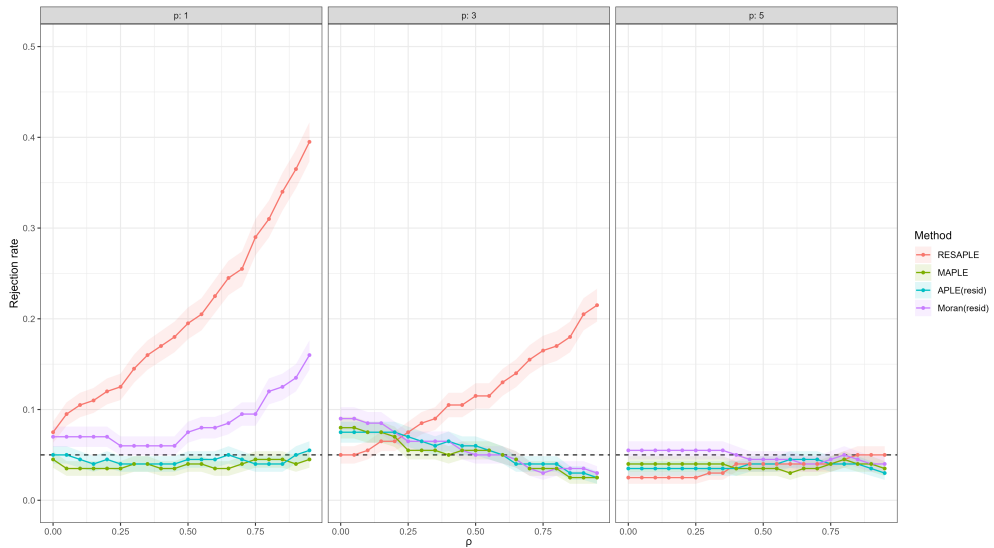
where data were generated from the Gaussian SEM. The design points in this simulation are exactly the same as Simulation 1 (Table 1). We present the results for $\rho > 0$ below for simplicity.

For each replicate, we obtain p -values by permutation using the Freedman-Lane procedure ((Freedman and Lane, 1983)). We use $L = 199$ permutations per replicate, yielding a minimum attainable p -value of $1/(L + 1) = 0.005$,

which provides adequate resolution at $\alpha = 0.05$ while keeping computation feasibility over the full factorial grid. For each design point and each value of ρ , we ran 1000 independent permutation tests per seed, and used two seeds. We then pool results by averaging rejection rates across the two seeds.



(a) Power curves on $m \times m$ lattice grids, for varying (n, p) .



(b) Power curves on B07, varying p .

Figure 5: Power curves for (a) queen contiguity and (b) B07 contiguity across design points outlined in Table 1. The test size $\alpha = 0.05$ is dashed in black horizontally on the plots.

Figure 5 reports empirical rejection rates (empirical probability that the test rejects the null for our chosen significance level of $\alpha = 0.05$) as a function of ρ . Across the design points, the tests are well-calibrated at $\rho = 0$ (rejection rates near α). For $\rho > 0$, RESAPLE typically achieves higher rejection rates than the alternatives, indicating higher power. The advantage is most pronounced when the effective residual dimension $r = n - p$ is small (e.g., $n = 25$ with $p = 5$ or $p = 20$) and under the irregular B07 topology, where the gap between RESAPLE and Moran/APLE/MAPLE widens as ρ gets larger, particularly for smaller p . The exception is when $p = 5$ in 5b, where all

methods are equally deficient. However, that is a function of the fact that the residual space has very low degrees of freedom ($r = 3$), making it uninformative for ρ ; hence the tests are conservative.

6.3. Simulation 3: RESAPLE Tests Under Various Weight Matrices

In Simulation 3 we fix RESAPLE as a test statistic, and vary only the *testing procedure* and the choice of spatial weights W . The data-generating mechanism (Gaussian SEM), covariates, and design of this simulation match simulations 1 and 2. The goal is to isolate how the choice of W and choice of calibration method (exact, permutation, asymptotic z , see 4.1) affect (i) empirical size at $\rho = 0$ and (ii) power under $\rho > 0$, and to assess how well $\mathcal{I}_r(0)$ performs as a predictor of power (as suggested by Theorem 5.1).

On the $m \times m$ lattices we considered multiple candidate weight matrices: rook and queen contiguity, and symmetrised k nearest neighbour (kNN) graphs with $k \in \{4, 6, 8\}$. The k nearest neighbour graphs were symmetrised by taking the union of directed neighbour relations, yielding an undirected graph. All weights were row-standardised. As in simulation 2, permutation tests use $L = 199$ permutations per replicate and we run $K = 2000$ Monte Carlo replicates per design point.

Figure 6 plots empirical power at a fixed alternative $\rho = 0.3$ against the corresponding $\mathcal{I}_r(0)$ value induced by each candidate W .

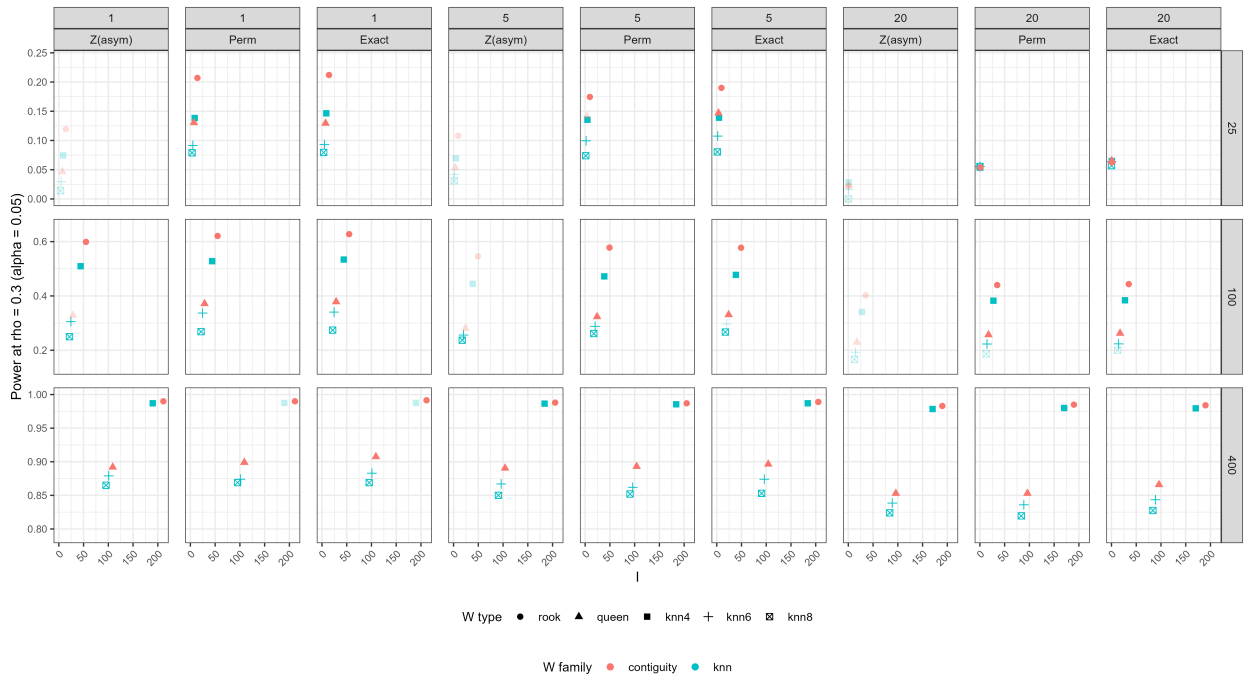
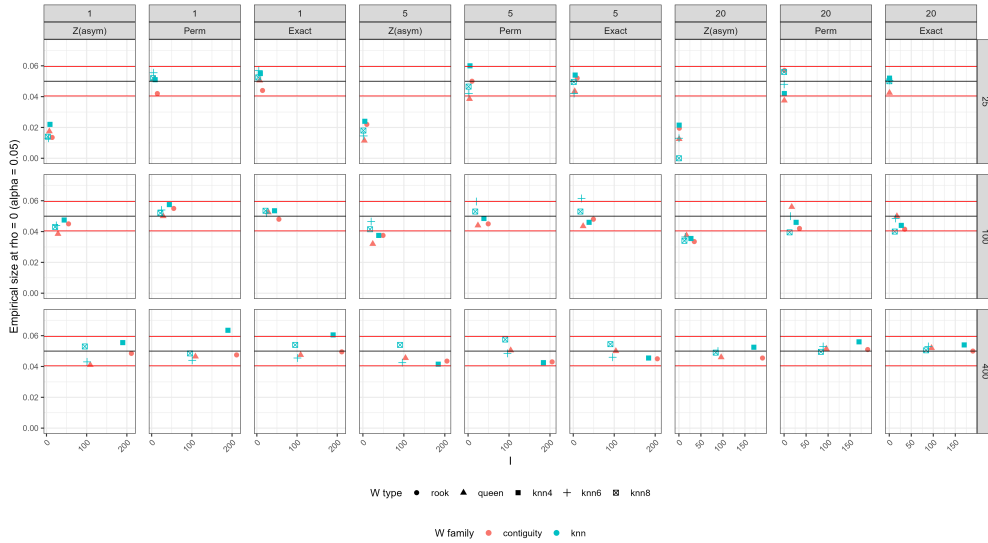


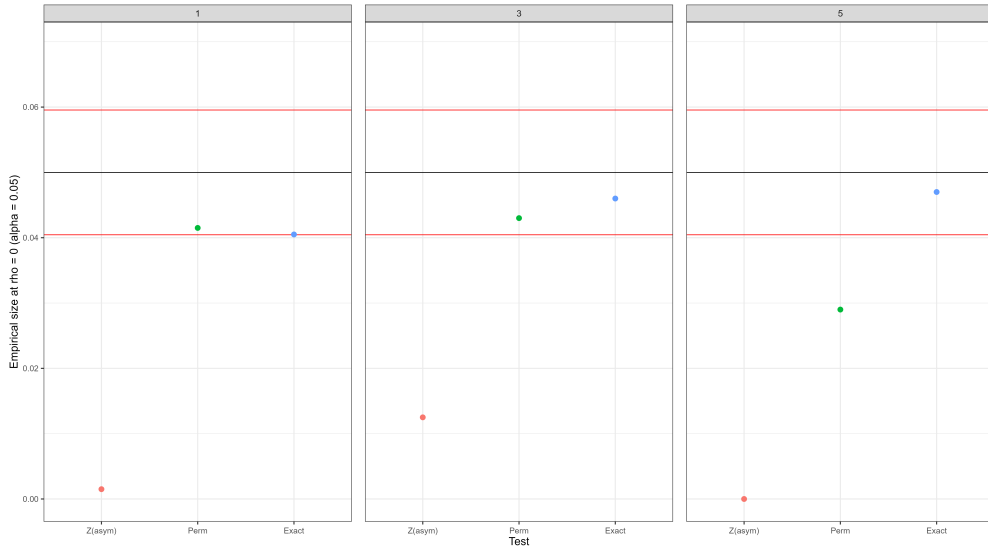
Figure 6: Empirical power at fixed $\rho = 0.3$ versus $\mathcal{I}_r(0)$ for different weight matrix W candidates. Panels are faceted by (n, p) and by testing procedure: rows correspond to $n \in \{25, 100, 400\}$, columns are grouped by $p \in \{1, 5, 20\}$ and then split into the three calibration methods (asymptotic z , permutation, and Gaussian exact). Each point shape corresponds to a particular W candidate, where faded points indicate W -procedure combinations that fail empirical size (defined as $|\widehat{\text{size}} - \alpha| > 0.01$).

It is clear from Figure 6 that for each design point (n, p) , power increases monotonically with $\mathcal{I}_r(0)$, showing that $\mathcal{I}_r(0)$ is an effective within-design predictor of detectability for RESAPLE at moderate dependent. In particular, weight choices with larger $\mathcal{I}_r(0)$ tend to yield higher power at $\rho = 0.3$, consistent with the local-information argument in Theorem 5.1. The fact that this ordering appears across procedures, especially permutation and exact, supports using $\mathcal{I}_r(0)$ as a practical diagnostic for choosing W when size is controlled. Although we display this for $\rho = 0.3$ as a representative case, this is generally true for small to moderate ρ , as the properties of our statistic follow local asymptotic theory (to the null). Indeed, the exception is at the null, where $\rho = 0$, as seen in Figure 7.

RESAPLE



(a) W Candidates on $m \times m$ lattice grid.



(b) Adjacency on B07.

Figure 7: Empirical size (rejection rate under H_0) at fixed $\rho = 0$ versus $\mathcal{I}_r(0)$ for different weight matrix W candidates. The black line indicates $\alpha = 0.05$ and the red bands indicate $\alpha \pm 1.96 \widehat{SE}$.

Figure 7 repeats the same experiment under the null $\rho = 0$. We observe clearly that at $\rho = 0$, $\mathcal{I}_r(0)$ generally has no explanatory power on rejection rates, which makes sense because in principle, each test should reject at the $\alpha = 0.05$ rate under the null. For almost all design points and each test, the points are within the 95% Monte Carlo bands (in red). The main departures occur for the asymptotic z-test, particularly when n is small or there is small $R = n - p$ (Figure 7a). Here, z-testing is far too conservative, which makes sense as approximate z-testing is an asymptotic test. It is worth noting that for B07 (Figure 7b), which is the canonical pathological case, the only test that maintains size across all design points is the Gaussian exact test, which behaves as expected under the correctly specified Gaussian SEM (especially in small sample or irregular settings where asymptotic approximations are least trustworthy). This is in line with the discussion in Section 5 and Theorem D.1: when the effective dimension is small or the spectrum is irregular, exact or permutation-based reference distributions are preferable to a normal approximation.

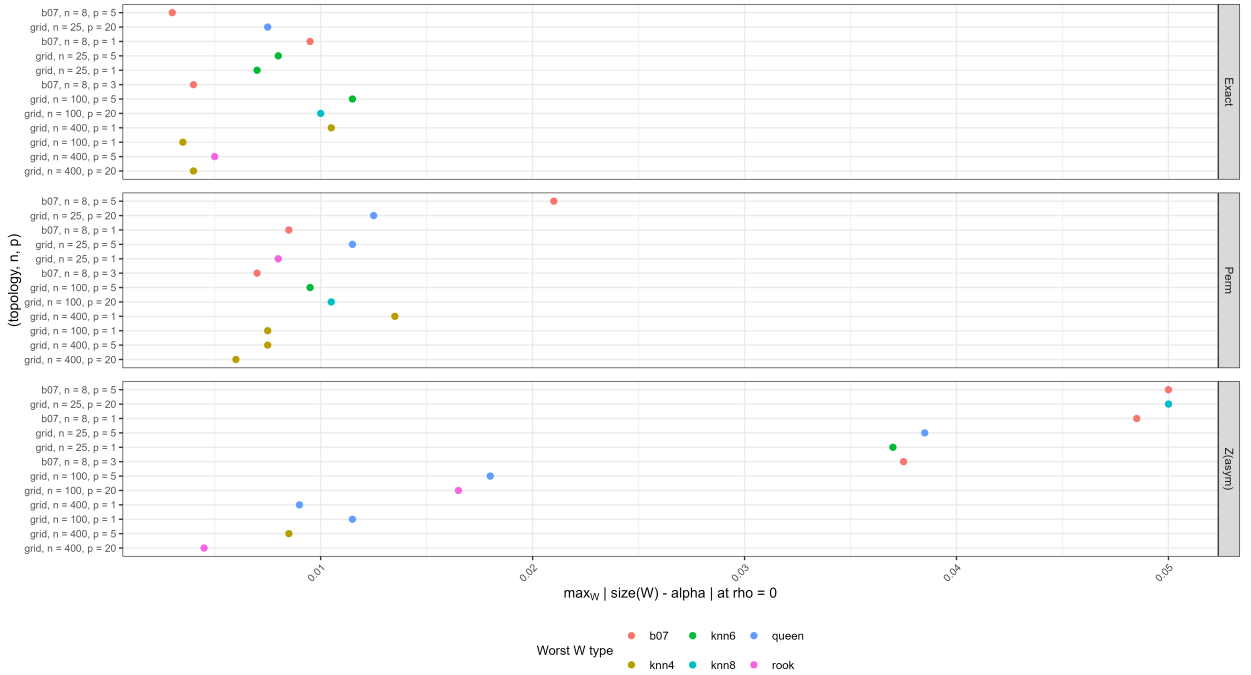


Figure 8: For each (topology, n , p) combination, we look at which W causes the worst size distortion. The x -axis is the error $\max_W |\widehat{\text{size}}(W) - \alpha|$ at $\rho = 0$. Points are the different weight matrices W . Note that for B07, there is exactly once choice of W – the adjacency matrix.

This observation can be generalised beyond the B07 topology. Figure 8 summarises worst-case size error across the candidate weight matrices for each design point and each testing procedure. It shows that the only test that consistency fails to maintain size is the approximate z-test. Since permutation testing is distribution free and usually maintains size in the same way as a Gaussian exact test, it lends credence to the fact that permutation testing is the most robust testing option in general as evidenced by much smaller worst-case deviations. The only possible exceptions are under challenging settings with irregular topology, n is small and large p (i.e. rightmost grid in Figure 7b). Of course in all possible cases, if the data is truly generated from a Gaussian SEM, the Gaussian exact test is optimal.

Finally, Figure 9 compares power curves for the three RESAPLE calibration methods. For the lattice designs (Figure 9a), we first selected a weight matrix W from the candidate set by maximising permutation-test power at $\rho = 0.3$ subject to the size constraint $|\widehat{\text{size}} - \alpha| \leq 0.01$, and then report the resulting power curves for all three procedures. For moderate-to-large n , the three calibrations give very similar power, with the Gaussian exact test typically slightly higher. In small n or small r scenarios, the asymptotic z-test can be substantially less powerful, consistent with its size distortions. The B07 curves (Figure 9b) further highlight this. We observe the exact calibration is most powerful under the correctly specified Gaussian SEM, permutation is competitive, and the z-approximation can be markedly conservative when r is small.

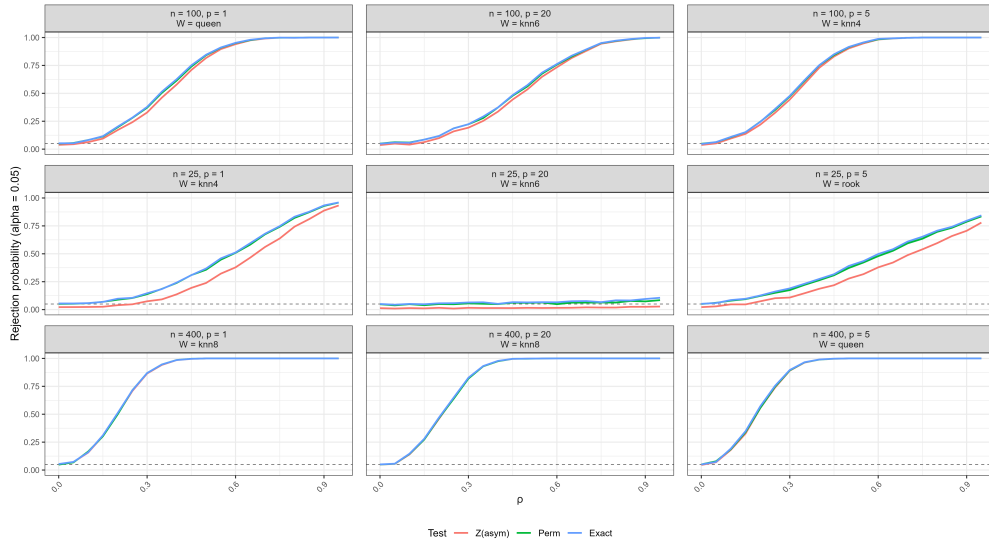
7. Real Data Case Study

We illustrate the usage of RESAPLE on a real areal dataset consisting of U.S. Census tracts in King County, Washington (USA). For each tract, we obtained 2019–2023 American Community Survey (ACS) 5-year estimates for median household income and tract-level demographic and socioeconomic covariates², and we merged these attributes with tract polygons³. Both of the data and geometries were obtained conveniently from the `tidycensus` package in R (Walker and Herman, 2017). The ACS 5-year product provides model-based small-area estimates with associated

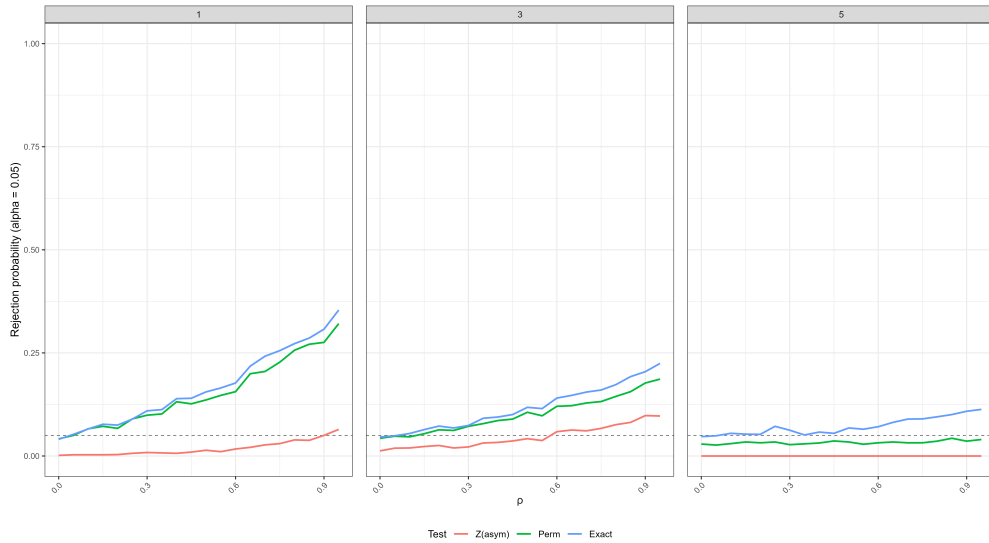
²<https://www.census.gov/data/developers/data-sets/acs-5year.html>

³<https://www.census.gov/geographies/mapping-files/time-series/geo/tiger-line-file.html>

RESAPLE



(a) Power curves for all three testing procedures on an $m \times m$ lattice. For a design point, W is chosen to maximise power for the permutation test at $\rho = 0.3$, while also maintaining size at $\rho = 0$.



(b) Power curves on B07 adjacency for all three testing procedures.

Figure 9: Power curves across design points.

margins of error; in this case study we treat the published estimates as observed inputs for the purpose of demonstrating spatial-residual diagnostics.

We examine natural log transformed median household income (MHHI) $Z_i = \log(\text{MHHI}_i)$ for census tract $i = 1, \dots, n$ ($n = 494$) in King County constructed from ACS table B19013. A map is provided in Appendix F. Covariates p include: 1) the share of adults with at least a bachelor's degree (constructed from educational-attainment counts), 2) unemployment rate, 3) renter share, 4) median age, 5) poverty rate, and 6) household vacancy rate. Variables were joined by tract GEOID.

The objective of our analysis is to understand how Z_i varies spatially. Recall that our model assumption is that

$$Z = X\beta + U, \quad U = \rho WU + \epsilon.$$

Model	Mean structure for Z_i (additive terms in $\eta_i = x_i^\top \beta$)
M0	Intercept only: 1
M1	1 + bach_plus + unemp + renter + age
M2	M1 + poverty + vacancy
M3	M2 + cx_s + cy_s
M4	M3 + cx_s ² + cy_s ² + (cx_s · cy_s)

Table 2

Model ladder used in the case study. cx_s, cy_s denote standardized tract-centroid (x, y) coordinates; M4 augments the linear spatial trend with quadratic terms to capture smooth large-scale spatial gradients.

Model	p	W	$I_r(0)$	Moran	APLE	MAPLE	RESAPLE	REML
M0	1	knn4	215.3634	0.5837950	0.6823412	0.6850960	0.6888040	0.7031737
M1	5	knn4	209.2293	0.3800045	0.5113108	0.5349882	0.5393361	0.5518016
M2	7	knn4	206.5113	0.1871191	0.3261134	0.3596274	0.3581660	0.4249890
M3	9	knn4	202.9122	0.1462524	0.2724848	0.3112651	0.3173588	0.4039653
M4	12	knn4	198.0635	0.1260997	0.2427351	0.2803249	0.2996965	0.3906761

Table 3

Global dependence summaries across the model ladder. p is the number of columns in X (including the intercept). W is the chosen candidate weights matrix (here knn4). $I_r(0)$ denotes the restricted null information used for W selection. Moran is computed on OLS residuals; APLE, MAPLE, and RESAPLE are one-step estimators; REML is the maximiser of the restricted profile likelihood over ρ .

The spatial error component U is shared regardless of the mean model, all we have to do is specify the mean structure $X\beta$, and then assess whether residual spatial autocorrelation persists in U . Although RESAPLE accounts for covariates through the restricted likelihood, it does so conditional on a chosen design matrix X , so changing X changes what is treated as trend versus “residual dependence.” Because there is no uniquely correct detrending specification in practice, we used a “ladder” approach of increasing linear mean model flexibility to assess sensitivity of spatial residual diagnostics to the extent of covariate adjustment. Specifically we consider the sequence of linear predictors described in Table 2, ranging from intercept only (M0) through socioeconomic covariates (M1-M2) and finally adding spatial trend with centroid coordinates (M3-M4). The main reason we do this is to compare how RESAPLE behaves compared to alternatives with increasing p (and hence changing $r = n - p$).

For each specification of design matrix X , we computed the OLS residuals $r = M_X Z$ and applied global and local spatial diagnostics to assess whether residual spatial autocorrelation persisted after adjustment. This required specifying a spatial weights matrix W , which is typically not uniquely determined (Section 5). We considered a broad candidate set $\mathcal{W} = \{\text{rook, queen, knn4, knn6, knn8}\}$. For each (X, W) pair we computed $I_r(0)$ and selected W by maximising the information over \mathcal{W} . Using the selected W we then report Moran’s I_M , APLE, MAPLE, RESAPLE, and the REML SEM estimate of ρ . The results are summarized in Table 3, and visualized in Figure 10.

In principle, because RESAPLE is derived as a one-step approximation to the REML score equation, it should track the REML estimate more closely than ML-based one-step alternatives when covariates are present. In Table 3 RESAPLE is indeed the closest one-step estimator to REML for M0, M1, M3, and M4. In M2, we see that MAPLE is marginally closer but the difference between MAPLE and RESAPLE is small relative to the gap between one-step estimators and REML overall. Although we do not have a ground truth ρ in this application, treating REML as a “model-based” gold-standard benchmark suggests that RESAPLE provides a particularly accurate closed-form dependence summary in the residual space. It is worth emphasising that this holds even though the estimated spatial dependence ρ is moderate rather than near zero, i.e. outside of the regime where one-step estimators are guaranteed to be most accurate. This provides credence to the claim that RESAPLE is more accurate than other ESDA indices on covariate-adjusted data.

Taking M4 as representative, we plotted the RESAPLE scatterplot and a map of the local RESAPLE contributions C_i in Figure 11. The scatterplot and the local plot generally describe the same story: most points have little leverage

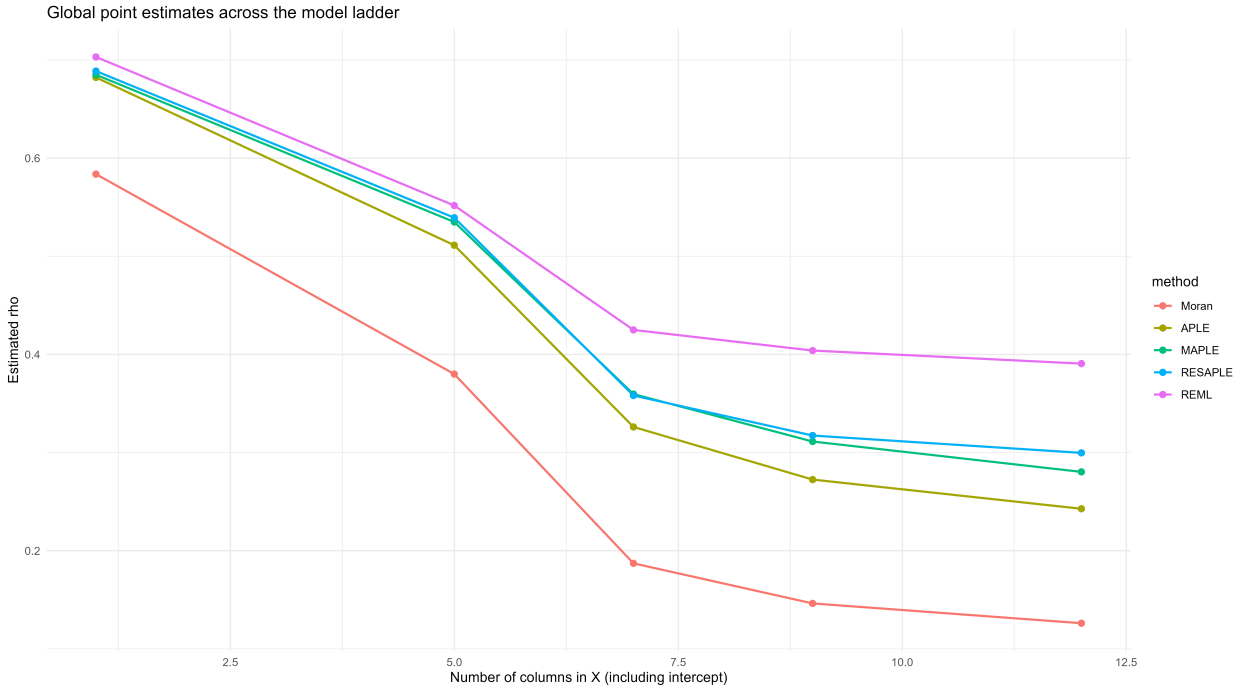
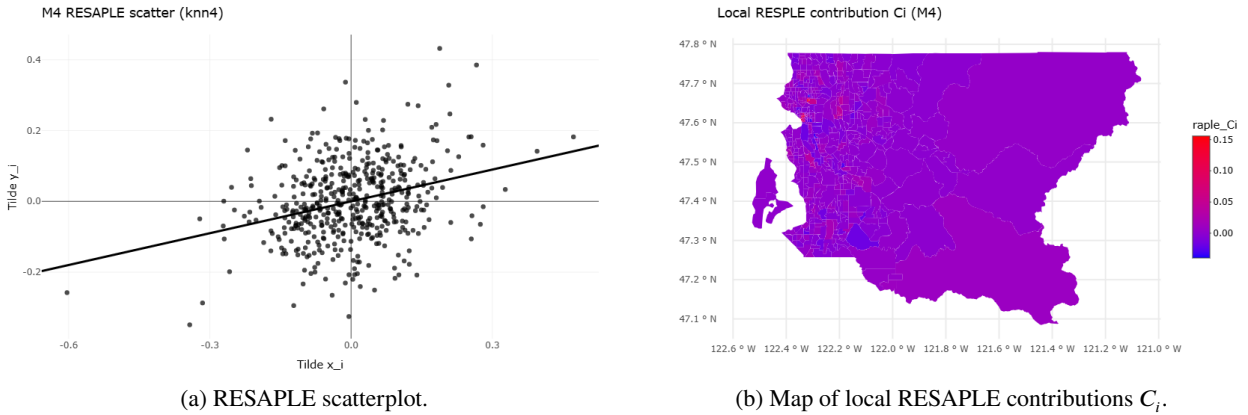


Figure 10: Method of ρ estimation via different estimators, by model, for 4NN W .



(a) RESAPLE scatterplot.

(b) Map of local RESAPLE contributions C_i .

Figure 11: Additional ESDA visualisations (scatterplot, local contributions) associated with the RESAPLE statistic for model M4.

on RESAPLE, which shows up on the map as most points having the same relative colour (around zero). The map generally matches our expectations. For instance, we would expect high-income areas such as Seattle to be an outlier, and indeed the locations that do have highest positive contribution on the scatterplot (and equivalently, redder colours on the local contribution map) are in the northwestern part of King County, which corresponds to the Seattle area. This shows that the ESDA products we obtain from RESAPLE also align with our desired properties.

8. Conclusion

In this paper, we introduced RESAPLE, a one-step restricted likelihood estimator for the spatial dependence parameter in Gaussian SEMs with covariates. RESAPLE preserves the computational and interpretive advantages of APLE-type statistics through a closed-form ratio of quadratic forms, while remaining invariant to reparameterisations

of the design matrix and to the choice of orthonormal residual basis. Most importantly, it targets the setting that dominates applied spatial statistical workflows: diagnosing and testing residual spatial dependence *after* detrending data via a mean model.

Beyond defining the estimator, we developed theory parallel to the ML-based APLE literature in the restricted likelihood setting. This framework yields an analytic expression for the restricted Fisher information at the null, $\mathcal{I}_r(0)$, which we use as a principled measure of local informativeness for comparing candidate spatial weight matrices after covariate adjustment. In this sense, the restricted-information perspective provides guidance for resolving a common practical ambiguity in spatial data analysis: how the choice of the spatial weight matrix W affects detectability of residual spatial dependence.

RESAPLE is primarily an ESDA tool. In our simulation studies, it is competitive with and often improves upon existing indices for summarising and testing residual spatial dependence across a range of sample sizes, covariate dimensions, and spatial topologies. We also demonstrated how RESAPLE can be used in practice for residual diagnostics, scatterplot visualization and mapping using a real data case study on median household income in King County, Washington, USA.

There are several other extensions that we may consider. First, it would be valuable to extend the restricted one-step construction to other spatial models, including SAR-lag specifications and models with additional variance components. Second, further work is needed to characterize robustness to distributional misspecification, heteroscedasticity, and uncertainty in small area estimates. Finally, while $\mathcal{I}_r(0)$ provides an analytic criterion for comparing candidate weights locally, developing a fully systematic weight selection strategy that balances power, calibration, and interpretability remains an important topic for future work.

Acknowledgements

Dr. Meredith Franklin's contributions to this work were supported by the Natural Sciences and Engineering Research Council of Canada (NSERC) RGPIN-2024-06444.

A. Additional Discussion of Section 2

A.1. Covariance Structure Under the Gaussian SEM

Recall the SEM

$$Z = X\beta + U, \quad U = \rho WU + \epsilon, \quad \epsilon \sim N(0, \sigma^2 I_n),$$

and write $R(\rho) = I_n - \rho W$. Under the standing assumption that $\det R(\rho) \neq 0$, we may solve the error equation to obtain

$$U = R(\rho)^{-1} \epsilon.$$

It follows immediately that

$$U \sim N(0, \sigma^2 R(\rho)^{-1} R(\rho)^{-\top}).$$

Consequently, the response satisfies

$$Z \sim N(X\beta, \sigma^2 \Sigma(\rho)), \quad \Sigma(\rho) = R(\rho)^{-1} R(\rho)^{-\top}.$$

A.2. Log-likelihood Under the Gaussian SEM

Let $\Sigma(\rho) = R(\rho)^{-1} R(\rho)^{-\top}$ so that $Z \sim N(X\beta, \sigma^2 \Sigma(\rho))$ and $\Sigma(\rho)^{-1} = R(\rho)^\top R(\rho)$. Moreover,

$$|\Sigma(\rho)| = |R(\rho)^{-1} R(\rho)^{-\top}| = |R(\rho)|^{-2}.$$

Therefore, up to the constant $C_n = -\frac{n}{2} \log(2\pi)$, the Gaussian log-likelihood is

$$\begin{aligned} \ell(\beta, \rho, \sigma^2) &= C_n - \frac{1}{2} \log |\sigma^2 \Sigma(\rho)| - \frac{1}{2} (Z - X\beta)^\top (\sigma^2 \Sigma(\rho))^{-1} (Z - X\beta) \\ &= C_n + \log |R(\rho)| - \frac{n}{2} \log \sigma^2 - \frac{1}{2\sigma^2} (Z - X\beta)^\top R(\rho)^\top R(\rho) (Z - X\beta). \end{aligned}$$

A.3. The SEM as a Gaussian LMM and the REML Viewpoint

The SEM can be viewed as a Gaussian linear model with a covariance parameter. Specifically, the representation

$$Z = X\beta + U, \quad U \sim N(0, \sigma^2 \Sigma(\rho))$$

shows that (ρ, σ^2) act as variance parameters governing the covariance structure of the errors. This motivates the usage of the standard restricted maximum likelihood (REML) framework for Gaussian models with fixed effects, as our ultimate goal is to do inference on the variance components of the model. In particular, REML eliminates β by basing inference for (ρ, σ^2) on linear combinations of Z that remove the contribution of X , which aligns with the standard of detrending data before conducting ESDA.

For completeness, we recall the residual-space construction. Let

$$P = X(X^\top X)^{-1}X^\top, \quad M = I_n - P,$$

and let $H \in \mathbb{R}^{n \times r}$, $r = n - p$, satisfy $H^\top H = I_r$ and $HH^\top = M$. The residualised contrasts are $e = H^\top Z$.

A.4. Proof of Lemma 2.1

Proof. For the first point, note that $MX = 0$ by definition of M . Since $HH^\top = M$, we have $HH^\top X = MX = 0$. Multiplying on the left by H^\top and using $H^\top H = I_r$ yields

$$H^\top X = H^\top HH^\top X = H^\top (HH^\top X) = 0.$$

Therefore,

$$e = H^\top Z = H^\top (X\beta + U) = H^\top X\beta + H^\top U = H^\top U.$$

For the second point, noting that $U = R(\rho)^{-1}\epsilon$, we have

$$e = H^\top U = H^\top R(\rho)^{-1}\epsilon.$$

Since $\epsilon \sim N(0, \sigma^2 I_n)$ and $H^\top R(\rho)^{-1}$ is deterministic conditional on (X, W) , it follows that e is Gaussian with mean zero and covariance

$$\begin{aligned} \text{Cov}(e) &= \sigma^2 H^\top R(\rho)^{-1} I_n R(\rho)^{-\top} H \\ &= \sigma^2 H^\top R(\rho)^{-1} R(\rho)^{-\top} H = \sigma^2 \Sigma_r(\rho), \end{aligned}$$

where $\Sigma_r(\rho) = H^\top R(\rho)^{-1} R(\rho)^{-\top} H$. □

B. Additional Discussion of Section 3

B.1. Restricted Likelihood and Profiling

Lemma B.1. *Under the SEM model, the restricted likelihood for (ρ, σ^2) up to an additive constant is*

$$\ell_r(\rho, \sigma^2; Z) = \log |R(\rho)| - \frac{1}{2} \log |X^\top R(\rho)^\top R(\rho) X| - \frac{r}{2} \log \sigma^2 - \frac{1}{2\sigma^2} Z^\top P_{R^\top(\rho)R(\rho)} Z,$$

where

$$P_{R^\top(\rho)R(\rho)} = R(\rho)^\top R(\rho) - R(\rho)^\top R(\rho) X (X^\top R(\rho)^\top R(\rho) X)^{-1} X^\top R(\rho)^\top R(\rho).$$

Equivalently in terms of the residual contrasts $e = H^\top Z$, we may write

$$\ell_r(\rho, \sigma^2; e) = C_r - \frac{r}{2} \log \sigma^2 - \frac{1}{2} \log |\Sigma_r(\rho)| - \frac{1}{2\sigma^2} e^\top \Sigma_r(\rho)^{-1} e,$$

where $\Sigma_r(\rho) = H^\top R(\rho)^{-1} R(\rho)^{-\top} H$ as in Lemma 2.1, and C_r is an additive constant that does not depend on (ρ, σ^2) .

Proof. Let $V(\rho, \sigma^2) = \sigma^2 \Sigma(\rho) = \sigma^2 R(\rho)^{-1} R(\rho)^{-\top}$. For a Gaussian linear model $Z \sim N(X\beta, V)$ with V positive definite and X full rank, the restricted log-likelihood for the covariance parameters, up to an additive constant, is

$$\ell_R(V; Z) = -\frac{1}{2} \left(\log |V| + \log |X^\top V^{-1} X| + Z^\top P_V Z \right),$$

where

$$P_V = V^{-1} - V^{-1} X (X^\top V^{-1} X)^{-1} X^\top V^{-1}.$$

In our setting, $V^{-1} = \sigma^{-2} \Sigma(\rho)^{-1} = \sigma^{-2} R(\rho)^\top R(\rho)$, and $|V| = (\sigma^2)^n |\Sigma(\rho)|$. Since $|\Sigma(\rho)| = |R(\rho)^{-1} R(\rho)^{-\top}| = |R(\rho)|^{-2}$, we have

$$\log |V| = n \log \sigma^2 - 2 \log |R(\rho)|.$$

Moreover,

$$X^\top V^{-1} X = \sigma^{-2} X^\top R(\rho)^\top R(\rho) X, \quad \log |X^\top V^{-1} X| = -p \log \sigma^2 + \log |X^\top R(\rho)^\top R(\rho) X|.$$

Finally, $P_V = \sigma^{-2} P_{R^\top(\rho)R(\rho)}$. Substituting these identities into $\ell_R(V; Z)$ and simplifying yields our asserted form for $\ell_r(\rho, \sigma^2; Z)$, up to an additive constant. For the representation in terms of e , note from Lemma 2.1 that $e = H^\top Z$ is Gaussian with mean zero and covariance $\sigma^2 \Sigma_r(\rho)$, where $\Sigma_r(\rho) = H^\top R(\rho)^{-1} R(\rho)^{-\top} H$. The restricted likelihood is invariant (up to an additive constant not depending on (ρ, σ^2)) to replacing Z by any full-rank set of error contrasts that annihilate X ; hence it may be written as the Gaussian log-likelihood of e , which yields the stated form for $\ell_r(\rho, \sigma^2; e)$. \square

Lemma B.2. *For the restricted log-likelihood in e given by*

$$\ell_r(\rho, \sigma^2; e) = -\frac{r}{2} \log \sigma^2 - \frac{1}{2} \log |\Sigma_r(\rho)| - \frac{1}{2\sigma^2} e^\top \Sigma_r(\rho)^{-1} e,$$

the profile log-likelihood (up to additive constants) is

$$\ell_r^p(\rho; e) = -\frac{1}{2} \log |\Sigma_r(\rho)| - \frac{r}{2} \log \left(\frac{1}{r} e^\top \Sigma_r(\rho)^{-1} e \right).$$

Proof. Differentiating $\ell_r(\rho, \sigma^2; e)$ with respect to σ^2 yields

$$\frac{\partial}{\partial \sigma^2} \ell_r(\rho, \sigma^2; e) = -\frac{r}{2\sigma^2} + \frac{1}{2\sigma^4} e^\top \Sigma_r(\rho)^{-1} e.$$

Setting this derivative to zero and solving yields

$$\hat{\sigma}_r^2(\rho) = \frac{1}{r} e^\top \Sigma_r(\rho)^{-1} e.$$

Substituting $\hat{\sigma}_r^2(\rho)$ into $\ell_r(\rho, \sigma^2; e)$ and collecting terms gives the stated profile likelihood, up to an additive constant. \square

B.2. Proof of Lemma 3.1

Proof. For the first point, at $\rho = 0$ we have $R(0) = I_n$ and therefore $\Sigma(0) = I_n$. Hence $\Sigma_r(0) = H^\top I_n H = I_r$.

For the second point, note that $(I_n - \rho W)^{-1} = I_n + \rho W + \mathcal{O}(\rho^2)$ as $\rho \rightarrow 0$. Therefore,

$$\begin{aligned} \Sigma(\rho) &= R(\rho)^{-1} R(\rho)^{-\top} = (I_n + \rho W + \mathcal{O}(\rho^2)) (I_n + \rho W^\top + \mathcal{O}(\rho^2)) \\ &= I_n + \rho(W + W^\top) + \mathcal{O}(\rho^2), \end{aligned}$$

so that $\Sigma'(0) = W + W^\top$. It follows that

$$\Sigma'_r(0) = H^\top \Sigma'(0) H = H^\top (W + W^\top) H = W_r + W_r^\top = 2K_r.$$

For the third point, write $Q(\rho) = e^\top \Sigma_r(\rho)^{-1} e$, so that

$$\ell_r^\rho(\rho; e) = -\frac{1}{2} \log |\Sigma_r(\rho)| - \frac{r}{2} \log Q(\rho) + \text{const.}$$

Then

$$S_r(\rho) = -\frac{1}{2} \frac{\partial}{\partial \rho} \log |\Sigma_r(\rho)| - \frac{r}{2} \frac{\partial}{\partial \rho} \log Q(\rho).$$

Using $\frac{\partial}{\partial \rho} \log |\Sigma_r(\rho)| = \text{Tr}(\Sigma_r(\rho)^{-1} \Sigma_r'(\rho))$ gives $\frac{\partial}{\partial \rho} \log |\Sigma_r(\rho)| \Big|_{\rho=0} = \text{Tr}(2K_r)$. Moreover, we have that $\frac{\partial}{\partial \rho} \Sigma_r(\rho)^{-1} = -\Sigma_r(\rho)^{-1} \Sigma_r'(\rho) \Sigma_r(\rho)^{-1}$, so

$$Q'(0) = -e^\top \Sigma_r'(0) e = -2e^\top K_r e, \quad Q(0) = e^\top e,$$

and therefore

$$\frac{\partial}{\partial \rho} \log Q(\rho) \Big|_{\rho=0} = \frac{Q'(0)}{Q(0)} = -2 \frac{e^\top K_r e}{e^\top e}.$$

Substituting these identities into the expression for $S_r(\rho)$ yields

$$S_r(0) = -\text{Tr}(K_r) + r \frac{e^\top K_r e}{e^\top e}.$$

□

B.3. Proof of Theorem 3.3

Proof. We prove each point in turn.

For the first point, let \tilde{H} be another choice satisfying $\tilde{H}\tilde{H}^\top = M$, $\tilde{H}^\top \tilde{H} = I_r$, and $\tilde{H}^\top X = 0$. Then there exists an orthogonal matrix $Q \in \mathbb{R}^{r \times r}$ such that $\tilde{H} = HQ$. Define

$$\tilde{e} = \tilde{H}^\top Z = Q^\top e, \quad \tilde{W}_r = \tilde{H}^\top W \tilde{H} = Q^\top W_r Q, \quad \tilde{K}_r = \frac{1}{2}(\tilde{W}_r + \tilde{W}_r^\top) = Q^\top K_r Q.$$

The trace is cyclic, so it immediately follows that $\text{Tr}(\tilde{K}_r) = \text{Tr}(K_r)$ and $\text{Tr}(\tilde{W}_r^2) = \text{Tr}(W_r^2)$, so μ_r and ν_r are unchanged. Moreover,

$$\tilde{e}^\top (\tilde{K}_r - \mu_r I_r) \tilde{e} = e^\top Q(Q^\top K_r Q - \mu_r I_r) Q^\top e = e^\top (K_r - \mu_r I_r) e,$$

and similarly $\tilde{e}^\top (\tilde{W}_r^\top \tilde{W}_r + \nu_r I_r) \tilde{e} = e^\top (W_r^\top W_r + \nu_r I_r) e$. This proves invariance to the choice of H .

For the second point, under $\rho = 0$ the model reduces to $Z = X\beta + \epsilon$ with $\epsilon \sim N(0, \sigma^2 I_n)$, so $e = H^\top \epsilon \sim N(0, \sigma^2 I_r)$. Note $\mathbb{E}_0[e^\top A e] = \sigma^2 \text{Tr}(A)$. Taking $A = K_r - \mu_r I_r$ and using $\mu_r = \text{Tr}(K_r)/r$ gives $\text{Tr}(A) = 0$ and hence $\mathbb{E}_0[e^\top (K_r - \mu_r I_r) e] = 0$. Taking $A = W_r^\top W_r + \nu_r I_r$ gives

$$\mathbb{E}_0[e^\top (W_r^\top W_r + \nu_r I_r) e] = \sigma^2 (\text{Tr}(W_r^\top W_r) + \nu_r r) = \sigma^2 (\text{Tr}(W_r^\top W_r) + \text{Tr}(W_r^2)),$$

which is strictly positive whenever $K_r \neq 0$ (equivalently, whenever $\text{Tr}(K_r^2) > 0$).

For the third and fourth points, consider the one-step approximation to the restricted score equation at $\rho = 0$,

$$S_r(0) + \mathcal{I}_r^A(0)\rho = 0,$$

with $\mathcal{I}_r^A(0)$ as defined in Theorem 3.3. By Lemma 3.1,

$$S_r(0) = \frac{r}{e^\top e} e^\top (K_r - \mu_r I_r) e.$$

Hence,

$$-\frac{S_r(0)}{\mathcal{I}_r^A(0)} = -\frac{\frac{r}{e^\top e} e^\top (K_r - \mu_r I_r) e}{-\frac{r}{e^\top e} e^\top (W_r^\top W_r + \nu_r I_r) e} = \frac{e^\top (K_r - \mu_r I_r) e}{e^\top (W_r^\top W_r + \nu_r I_r) e} = \hat{\rho}_{\text{RESAPLE}},$$

which proves (3) and (4). □

B.4. Proof of Corollary 3.4

Proof. Let $\tilde{X} = XQ$ with Q invertible. Then $\text{Im}(\tilde{X}) = \text{Im}(X)$, so the orthogonal projectors satisfy $\tilde{P} = P$ and $\tilde{M} = M$. Any admissible \tilde{H} with $\tilde{H}\tilde{H}^\top = M$ and $\tilde{H}^\top\tilde{H} = I_r$, differs from H by an orthogonal transformation. The conclusion follows from the first point of Theorem 3.3. \square

B.5. Motivating the Approximate Curvature and Restricted Fisher Information

To motivate $\mathcal{I}_r^A(0)$, it is helpful to discuss the Fisher information for a covariance parameter in a mean zero Gaussian model.

Lemma B.3. *Let $y \sim N(0, C(\theta))$ where $C(\theta)$ is positive definite and twice continuously differentiable in $\theta \in \mathbb{R}$. Then the Fisher information for θ is*

$$\mathcal{I}(\theta) = \frac{1}{2} \text{Tr} \left(C(\theta)^{-1} C_\theta(\theta) C(\theta)^{-1} C_\theta(\theta) \right),$$

where $C_\theta(\theta) = \frac{\partial}{\partial \theta} C(\theta)$.

Proof. The log-likelihood is $\ell(\theta; y) = -\frac{1}{2} \log |C(\theta)| - \frac{1}{2} y^\top C(\theta)^{-1} y + \text{const}$. The score is

$$S(\theta; y) = \frac{\partial}{\partial \theta} \ell(\theta; y) = -\frac{1}{2} \text{Tr} (C^{-1} C_\theta) + \frac{1}{2} y^\top C^{-1} C_\theta C^{-1} y,$$

and $\mathbb{E}_\theta[S(\theta; y)] = 0$. For a zero mean Gaussian vector, $\text{Var}(y^\top A y) = 2 \text{Tr}(A C A C)$ for any deterministic, symmetric A . Taking $A = \frac{1}{2} C^{-1} C_\theta C^{-1}$ yields

$$\text{Var} (S(\theta; y)) = \frac{1}{4} \text{Var} (y^\top C^{-1} C_\theta C^{-1} y) = \frac{1}{2} \text{Tr} (C^{-1} C_\theta C^{-1} C_\theta),$$

which equals the Fisher information. \square

Lemma B.4. *For $e = H^\top Z$ under the SEM model, let $C(\rho) = \sigma^2 \Sigma_r(\rho)$. Then the Fisher information for ρ at $\rho = 0$ is*

$$\mathcal{I}_r(0) = 2 \text{Tr}(K_r^2) = \text{Tr}(W_r^\top W_r) + \text{Tr}(W_r^2).$$

Proof. By Lemma B.3,

$$\mathcal{I}_r(0) = \frac{1}{2} \text{Tr} \left(C(0)^{-1} C_\rho(0) C(0)^{-1} C_\rho(0) \right).$$

Using $C(0) = \sigma^2 I_r$ and $C_\rho(0) = \sigma^2 \Sigma_r'(0) = \sigma^2 (2K_r)$ gives

$$\mathcal{I}_r(0) = \frac{1}{2} \text{Tr} ((2K_r)^2) = 2 \text{Tr}(K_r^2).$$

Since $K_r = \frac{1}{2}(W_r + W_r^\top)$,

$$\begin{aligned} 4 \text{Tr}(K_r^2) &= \text{Tr}((W_r + W_r^\top)^2) = \text{Tr}(W_r^2) + \text{Tr}(W_r W_r^\top) + \text{Tr}(W_r^\top W_r) + \text{Tr}((W_r^\top)^2) \\ &= 2 \text{Tr}(W_r^2) + 2 \text{Tr}(W_r^\top W_r), \end{aligned}$$

and dividing by two yields $\mathcal{I}_r(0) = \text{Tr}(W_r^2) + \text{Tr}(W_r^\top W_r)$. \square

The expression $\mathcal{I}_r(0) = \text{Tr}(W_r^\top W_r) + \text{Tr}(W_r^2)$ provides an analytic characterization of the population curvature at $\rho = 0$. Denote the denominator of $\hat{\rho}_{RESAPLE}$ by

$$D(e) = e^\top (W_r^\top W_r + \nu_r I_r) e.$$

From Theorem 3.3, $\mathbb{E}_0[D(e)] = \sigma^2 \mathcal{I}_r(0)$. Since σ^2 is generally unknown, a natural estimator at $\rho = 0$ is $\hat{\sigma}_r^2(0) = \frac{1}{r} e^\top e$, and this motivates the curvature approximation

$$\mathcal{I}_r^A(0) = -\frac{r}{e^\top e} D(e),$$

which is approximately proportional to $-\mathcal{I}_r(0)$ after substituting $\hat{\sigma}_r^2(0) = \frac{1}{r} e^\top e$ for σ^2 , since $\frac{r}{e^\top e} \approx \frac{1}{\sigma^2}$ under $\rho = 0$ and $D(e) \approx \sigma^2 \mathcal{I}_r(0)$.

B.6. A Law of Large Numbers for Quadratic Forms

Lemma B.5. Let $e \sim N(0, \sigma^2 I_r)$ and let A_r be a sequence of deterministic symmetric $r \times r$ matrices with uniformly bounded operator norm. Then, as $r \rightarrow \infty$,

$$\frac{1}{r} \left(e^\top A_r e - \sigma^2 \text{Tr}(A_r) \right) \xrightarrow{p} 0.$$

Proof. We have $\mathbb{E}[e^\top A_r e] = \sigma^2 \text{Tr}(A_r)$ and $\text{Var}(e^\top A_r e) = 2\sigma^4 \text{Tr}(A_r^2)$. Uniform boundedness of $\|A_r\|_{op}$ implies $\text{Tr}(A_r^2) \leq r \|A_r\|_{op}^2 \leq Cr$ for some $C > 0$. Therefore,

$$\text{Var} \left(\frac{1}{r} (e^\top A_r e - \sigma^2 \text{Tr}(A_r)) \right) \leq \frac{2\sigma^4 C}{r} \rightarrow 0,$$

and the claim follows by Chebyshev's inequality. \square

Theorem B.6. Suppose that, as $r \rightarrow \infty$, the following hold:

1. $\sup_r \|W_r\|_{op} < \infty$,
2. $I_r(0)/r \rightarrow k > 0$.

Then

$$-\frac{I_r^A(0)}{I_r(0)} \xrightarrow{p} 1.$$

Proof. By Lemma B.5 with $A_r = I_r$, $(e^\top e)/(r\sigma^2) \xrightarrow{p} 1$, so $(r/e^\top e) \xrightarrow{p} 1/\sigma^2$. By Lemma B.5 with $A_r = W_r^\top W_r + \nu_r I_r$,

$$\frac{1}{r} \left(D(e) - \sigma^2 \text{Tr}(W_r^\top W_r + \nu_r I_r) \right) \xrightarrow{p} 0.$$

Since $\text{Tr}(W_r^\top W_r + \nu_r I_r) = \text{Tr}(W_r^\top W_r) + \text{Tr}(W_r^2) = I_r(0)$, we have $D(e)/(\sigma^2 I_r(0)) \xrightarrow{p} 1$, i.e. $D(e)/I_r(0) \xrightarrow{p} \sigma^2$. Therefore,

$$-\frac{I_r^A(0)}{I_r(0)} = \frac{r}{e^\top e} \cdot \frac{D(e)}{I_r(0)} \xrightarrow{p} \frac{1}{\sigma^2} \cdot \sigma^2 = 1.$$

\square

C. Additional Discussion of Section 4.1

Here we briefly review the exact Gaussian null distribution for $\hat{\rho}_{RESAPLE}$. Assume the Gaussian SEM and $H_0 : \rho = 0$, so that $e \sim N(0, \sigma^2 I_r)$. Define

$$A := K_r - \mu_r I_r, \quad B := W_r^\top W_r + \nu_r I_r,$$

so that $\hat{\rho}_{RESAPLE} = (e^\top A e)/(e^\top B e)$. Fix $t \in \mathbb{R}$. Provided B is symmetric positive definite (see Remark 4.1), the event $\{\hat{\rho}_{RESAPLE} \geq t\}$ is equivalent to

$$e^\top (A - tB) e \geq 0.$$

Let $C_t := A - tB$, and write the eigendecomposition $C_t = U_t \Lambda_t U_t^\top$, where U_t is orthogonal and $\Lambda_t = \text{diag}(\lambda_{t,1}, \dots, \lambda_{t,r})$.

Since $U_t^\top e \stackrel{d}{=} e$ under H_0 , one obtains

$$e^\top C_t e \stackrel{d}{=} \sum_{j=1}^r \lambda_{t,j} \sigma^2 \chi_{1,j}^2,$$

where $\chi_{1,1}^2, \dots, \chi_{1,r}^2$ are independent χ_1^2 random variables. Therefore,

$$\mathbb{P}_0(\hat{\rho}_{RESAPLE} \geq t) = \mathbb{P} \left(\sum_{j=1}^r \lambda_{t,j} \chi_{1,j}^2 \geq 0 \right).$$

One can evaluate the distribution function of such linear combinations of independent chi-square variables for instance, Imhof's method computes distribution functions by characteristic function inversion (Imhof, 1961). This is exact.

D. Additional Discussion of Section 5

D.1. Proof of Theorem 5.1

Proof. Recall that $K_r = H^\top K H$ with $H H^\top = M$ and $H^\top H = I_r$. Since K is symmetric and M is a symmetric idempotent projector,

$$\text{Tr}(K_r^2) = \text{Tr}(H^\top K H H^\top K H) = \text{Tr}(H H^\top K H H^\top K) = \text{Tr}(M K M K),$$

which yields (9).

We next prove (10). Since M is an orthogonal projector, the Frobenius norm is contractive under left and right multiplication by M . Hence

$$\text{Tr}(K_r^2) = \text{Tr}((M K M)^2) = \|M K M\|_F^2 \leq \|K\|_F^2 = \text{Tr}(K^2).$$

Multiplying by 2 gives $I_r(0) \leq 2 \text{Tr}(K^2)$. Finally, since $K = (W + W^\top)/2$,

$$2 \text{Tr}(K^2) = \frac{1}{2} \text{Tr}((W + W^\top)^2) = \text{Tr}(W^\top W) + \text{Tr}(W^2),$$

which proves (10).

We now derive (11) for $W = D^{-1}A$. Since $w_{ij} = a_{ij}/d_i$ and $a_{ij}^2 = a_{ij}$, we have

$$\text{Tr}(W^\top W) = \sum_{i=1}^n \sum_{j=1}^n w_{ij}^2 = \sum_{i=1}^n \sum_{j=1}^n \frac{a_{ij}}{d_i^2} = \sum_{i=1}^n \frac{d_i}{d_i^2} = \sum_{i=1}^n \frac{1}{d_i}.$$

Moreover,

$$\text{Tr}(W^2) = \sum_{i=1}^n (W^2)_{ii} = \sum_{i=1}^n \sum_{j=1}^n w_{ij} w_{ji} = \sum_{i=1}^n \sum_{j=1}^n \frac{a_{ij} a_{ji}}{d_i d_j}.$$

If $A = A^\top$, then each undirected edge $\{i, j\}$ contributes twice to the double sum, which yields $\text{Tr}(W^2) = 2 \sum_{\{i,j\} \in E} (d_i d_j)^{-1}$. If, further, $d_i = d$ for all i , then $\sum_i d_i^{-1} = n/d$ and $2 \sum_{\{i,j\} \in E} (d_i d_j)^{-1} = 2|E|/d^2 = (nd)/d^2 = n/d$, since $|E| = nd/2$. This gives $\text{Tr}(W^\top W) + \text{Tr}(W^2) = 2n/d$. \square

D.2. A Spectral Heuristic for the RESAPLE Sampling Distribution

To discuss heuristically how spectral structure can affect the finite-sample distribution of RESAPLE, it is useful to recall the corresponding fact for an ordinary Rayleigh quotient involving a symmetric matrix. Although the null law of RESAPLE is, in general, a *generalised* Rayleigh quotient rather than the ordinary quotient treated below, the result gives useful intuition for why eigenvalue dispersion and multiplicity can influence finite-sample behaviour. We therefore describe how the eigenvalues of a symmetric matrix control the sampling law in this simpler benchmark case.

Theorem D.1. *Let $g \sim N(0, I_r)$ with $r \geq 3$, and let $S \in \mathbb{R}^{r \times r}$ be symmetric with eigenvalues $\lambda_1, \dots, \lambda_r$. Define the Rayleigh quotient $T(g) := \frac{g^\top S g}{g^\top g}$. Then the distribution of $T(g)$ depends on S only through $(\lambda_1, \dots, \lambda_r)$. Moreover,*

$$\mathbb{E}[T(g)] = \frac{\text{Tr}(S)}{r}, \quad \text{Var}(T(g)) = \frac{2}{r(r+2)} \sum_{j=1}^r (\lambda_j - \bar{\lambda})^2, \quad \bar{\lambda} = \frac{1}{r} \sum_{j=1}^r \lambda_j.$$

In particular, $\text{Var}(T(g)) = 0$ if and only if S is a scalar multiple of the identity.

Proof. Write $S = Q \Lambda Q^\top$ with $\Lambda = \text{diag}(\lambda_1, \dots, \lambda_r)$ and Q orthogonal. Set $h := Q^\top g$. Since $g \sim N(0, I_r)$ and Q is orthogonal, we have $h \stackrel{d}{=} g$; hence

$$T(g) = \frac{g^\top Q \Lambda Q^\top g}{g^\top g} = \frac{h^\top \Lambda h}{h^\top h} = \sum_{j=1}^r \lambda_j \frac{h_j^2}{\sum_{\ell=1}^r h_\ell^2}.$$

Thus the law of $T(g)$ depends on S only through its eigenvalues.

Now let

$$W_j := \frac{h_j^2}{\sum_{\ell=1}^r h_\ell^2}, \quad j = 1, \dots, r.$$

Because h_1, \dots, h_r are iid standard Normal, the vector (W_1, \dots, W_r) has a Dirichlet $(\frac{1}{2}, \dots, \frac{1}{2})$ distribution, which yields

$$\mathbb{E}[W_i] = \frac{1}{r}, \quad \mathbb{E}[W_i^2] = \frac{3}{r(r+2)}, \quad \mathbb{E}[W_i W_j] = \frac{1}{r(r+2)} \quad (i \neq j).$$

Since $T(g) = \sum_{i=1}^r \lambda_i W_i$, we obtain

$$\mathbb{E}[T(g)] = \sum_{i=1}^r \lambda_i \mathbb{E}[W_i] = \frac{1}{r} \sum_{i=1}^r \lambda_i = \frac{\text{Tr}(S)}{r},$$

and

$$\begin{aligned} \mathbb{E}[T(g)^2] &= \sum_{i=1}^r \lambda_i^2 \mathbb{E}[W_i^2] + \sum_{i \neq j} \lambda_i \lambda_j \mathbb{E}[W_i W_j] \\ &= \frac{3}{r(r+2)} \sum_{i=1}^r \lambda_i^2 + \frac{1}{r(r+2)} \sum_{i \neq j} \lambda_i \lambda_j = \frac{1}{r(r+2)} \left(2 \sum_{i=1}^r \lambda_i^2 + \left(\sum_{i=1}^r \lambda_i \right)^2 \right) \\ &= \frac{1}{r(r+2)} \left(2 \text{Tr}(S^2) + \text{Tr}(S)^2 \right). \end{aligned}$$

Subtracting $\mathbb{E}[T(g)]^2 = \text{Tr}(S)^2/r^2$ gives

$$\text{Var}(T(g)) = \frac{2}{r(r+2)} \left(\text{Tr}(S^2) - \frac{\text{Tr}(S)^2}{r} \right),$$

and the equivalent eigenvalue form follows by expanding $\sum_j (\lambda_j - \bar{\lambda})^2$. Finally, $\text{Var}(T(g)) = 0$ holds if and only if $\lambda_1 = \dots = \lambda_r$, that is, S is a scalar multiple of I_r . \square

The theorem does not directly describe the null law of RESAPLE, but it does provide a useful spectral heuristic. In particular, when the relevant residualised operators have highly dispersed eigenvalues or large multiplicities, one should expect stronger finite-sample departures from a Gaussian approximation. This intuition is consistent with the behaviour we observe for small r and irregular neighbourhood structures, and it helps motivate the use of exact or permutation-based calibration in such settings.

E. Additional Details for Simulations

E.1. Weight Matrices and Grids

We use two classes of spatial weight matrices. For Queen contiguity, we endow it on a $m \times m$ integer lattice with coordinates

$$\text{coords}_i = (x_i, y_i) \in \{1, \dots, m\}^2,$$

where $n = m^2$. On the other hand, for the pathological case with B07, we use a 8×8 binary adjacency matrix (denoted B07), row standardised. Coordinates are provided for covariate construction using a unit-circle embedding,

$$\text{coords}_i = (\cos(2\pi(i-1)/8), \sin(2\pi(i-1)/8)), \quad i = 1, \dots, 8.$$

E.2. Covariates and Coefficient Specification

The design matrix X always includes an intercept. When $p \geq 2$, the second column is a standardised version of the x -coordinate with additive $N(0, 0.1^2)$ perturbation; when $p \geq 3$, the third column is constructed analogously from the y -coordinate. For $p \geq 4$, remaining columns are standardised independent Gaussian draws. We apply standardisation column-wise. The coefficients are fixed deterministically as

$$\beta_1 = 1, \quad \beta_j = \frac{0.6}{\sqrt{j-1}} \text{ for } j \geq 2,$$

which induces a decaying signal across non-intercept covariates. This also ensures that the variance of $X\beta$ does not scale with p .

F. Additional Details for the Case Study

F.1. Map of Z_i

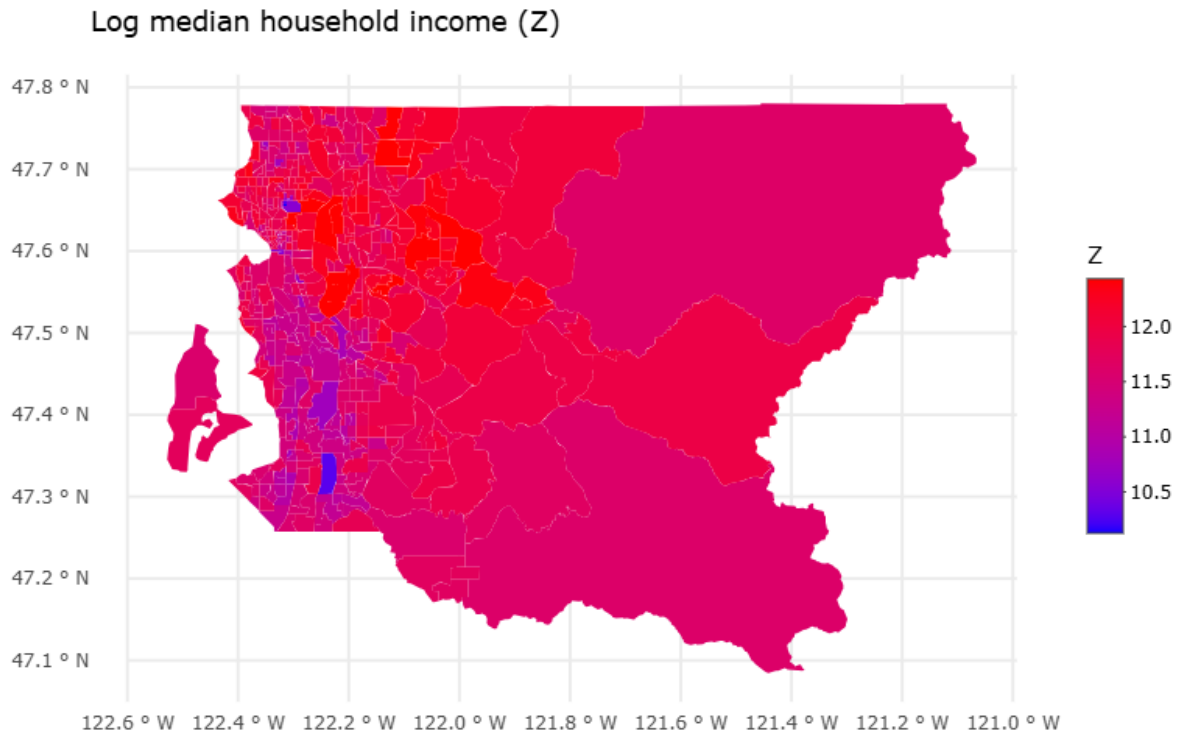


Figure 12: Map of Log Median Household Income.

F.2. Restricted Information for Each $W \in \mathcal{W}$

Table 4

Restricted null information across candidate weight matrices W , by model in the case study. Here $n = 494$ tracts and $n_{\text{iso}} = 0$ isolated units for all candidates. For each model, the selected W (maximising $I_r(0)$) is shown in **bold**. The ratio $\text{info_ratio} := I_r(0)/I_n(0)$ compares restricted to unrestricted null information, where $I_r(0) = 2\text{Tr}(MKMK)$ and $I_n(0) = 2\text{Tr}(K^2)$ with $K = (W + W^\top)/2$.

Model M0 ($p = 1$)			Model M1 ($p = 5$)			Model M2 ($p = 7$)		
W	avg_deg $I_r(0)$	$I_n(0)$ info_ratio	W	avg_deg $I_r(0)$	$I_n(0)$ info_ratio	W	avg_deg $I_r(0)$	$I_n(0)$ info_ratio
knn4	4.000000	217.5000	knn4	4.000000	217.5000	knn4	4.000000	217.5000
	215.36336	0.9901764		209.22927	0.9619737		206.51133	0.9494774
rook	5.356275	194.9016	rook	5.356275	194.9016	rook	5.356275	194.9016
	192.80485	0.9892422		187.10276	0.9599859		184.71094	0.9477140
queen	6.056680	173.4456	queen	6.056680	173.4456	queen	6.056680	173.4456
	171.34649	0.9878978		165.90602	0.9565308		163.67882	0.9436899
knn6	6.000000	146.4444	knn6	6.000000	146.4444	knn6	6.000000	146.4444
	144.34323	0.9856518		139.09374	0.9498055		137.05337	0.9358728
knn8	8.000000	110.7500	knn8	8.000000	110.7500	knn8	8.000000	110.7500
	108.66201	0.9811468		103.83073	0.9375235		102.13158	0.9221813

Model M3 ($p = 9$)			Model M4 ($p = 12$)		
W	avg_deg $I_r(0)$	$I_n(0)$ info_ratio	W	avg_deg $I_r(0)$	$I_n(0)$ info_ratio
knn4	4.000000	217.5000	knn4	4.000000	217.5000
	202.91220	0.9329296		198.06346	0.9106366
rook	5.356275	194.9016	rook	5.356275	194.9016
	181.19303	0.9296643		175.98054	0.9029201
queen	6.056680	173.4456	queen	6.056680	173.4456
	160.20081	0.9236374		155.01463	0.8937365
knn6	6.000000	146.4444	knn6	6.000000	146.4444
	133.69818	0.9129617		129.15404	0.8819320
knn8	8.000000	110.7500	knn8	8.000000	110.7500
	98.92989	0.8932722		94.53845	0.8536204

CRedit authorship contribution statement

Aditya Khan: Conceptualisation, Methodology, Software, Validation, Formal analysis, Investigation, Writing - Original Draft, Writing - Review & Editing, Visualisation. **Meredith Franklin:** Writing - Review & Editing, Supervision, Project Administration.

References

- Anselin, L., 1988. Lagrange Multiplier Test Diagnostics for Spatial Dependence and Spatial Heterogeneity. *Geogr. Anal.* 20, 1–17. doi:10.1111/j.1538-4632.1988.tb00159.x.
- Anselin, L., 1995. Local indicators of spatial association—lisa. *Geogr. Anal.* 27, 93–115. doi:10.1111/j.1538-4632.1995.tb00338.x.
- Anselin, L., Bera, A.K., Florax, R., Yoon, M.J., 1996. Simple diagnostic tests for spatial dependence. *Reg. Sci. Urban Econ.* 26, 77–104. doi:10.1016/0166-0462(95)02111-6.
- Freedman, D., Lane, D., 1983. A nonstochastic interpretation of reported significance levels. *J. Bus. Econ. Stat.* 1, 292–298. URL: <http://www.jstor.org/stable/1391660>.
- Gao, F., Languille, C., Karzazi, K., Guhl, M., Boukebous, B., Deguen, S., 2021. Efficiency of fine scale and spatial regression in modelling associations between healthcare service spatial accessibility and their utilization. *Int. J. Health Geogr.* 20, 22. doi:10.1186/s12942-021-00276-y.
- Harville, D.A., 1977. Maximum Likelihood Approaches to Variance Component Estimation and to Related Problems. *J. Am. Stat. Assoc.* 72, 320–338. doi:10.1080/01621459.1977.10480998.
- Imhof, J.P., 1961. Computing the distribution of quadratic forms in normal variables. *Biometrika* 48, 419–426. doi:10.1093/biomet/48.3-4.419, arXiv:<https://academic.oup.com/biomet/article-pdf/48/3-4/419/898067/48-3-4-419.pdf>.
- Jin, F., Lee, L.f., 2012. Approximated likelihood and root estimators for spatial interaction in spatial autoregressive models. *Reg. Sci. Urban Econ.* 42, 446–458. doi:10.1016/j.regsciurbeco.2011.12.004.
- Li, H., Calder, C.A., Cressie, N., 2007. Beyond Moran's I: Testing for Spatial Dependence Based on the Spatial Autoregressive Model. *Geogr. Anal.* 39, 357–375. doi:10.1111/j.1538-4632.2007.00708.x.
- Li, H., Calder, C.A., Cressie, N., 2012. One-step estimation of spatial dependence parameters: Properties and extensions of the APLE statistic. *J. Multivar. Anal.* 105, 68–84. doi:10.1016/j.jmva.2011.08.006.
- Moran, P.A.P., 1950. Notes on Continuous Stochastic Phenomena. *Biometrika* 37, 17–23. doi:10.1093/biomet/37.1-2.17.
- Patterson, H.D., Thompson, R., 1971. Recovery of inter-block information when block sizes are unequal. *Biometrika* 58, 545–554. doi:10.1093/biomet/58.3.545.
- Reder, M., Müller, W., 2009. More on the APLE statistic. *Math. Slovaca* 59, 565–578. doi:10.2478/s12175-009-0148-x.
- van der Vaart, A.W., 1998. *Asymptotic Statistics*. Cambridge Series in Statistical and Probabilistic Mathematics, Cambridge University Press, Cambridge. doi:10.1017/CB09780511802256.
- Ver Hoef, J.M., Peterson, E.E., Hooten, M.B., Hanks, E.M., Fortin, M.J., 2018. Spatial autoregressive models for statistical inference from ecological data. *Ecol. Monogr.* 88, 36–59. doi:10.1002/ecm.1283.
- Walker, K., Herman, M., 2017. *Tidycensus: Load US Census Boundary and Attribute Data as 'tidyverse' and 'sf'-Ready Data Frames*. doi:10.32614/CRAN.package.tidycensus.
- Wellner, J.A., . Chapter 4: Efficient likelihood estimation and related tests. *STAT 581 lecture notes*, University of Washington. URL: <https://sites.stat.washington.edu/jaw/COURSES/580s/581/LECTNOTES/ch4-rev1.pdf>. version: ch4-rev1. Accessed 2025-12-29.
- Zhang, X., Yu, J., 2018. Spatial weights matrix selection and model averaging for spatial autoregressive models. *J. Econom.* 203, 1–18. doi:10.1016/j.jeconom.2017.05.021.